Synthesis of a New Pyridine-Stretched Nucleoside

Wei Li

Master of Philosophy

ASTON UNIVERSITY

AUGUST 2002

ASTON UNIVERSITY

Synthesis of a New Pyridine-Stretched Nucleoside

Wei Li
Master of Philosophy 2002

SUMMARY

Synthetic oligonucleotides have potential, clinical usefulness for controlling gene expression at the DNA level. Inhibition of gene expression at the DNA level can be achieved by using triplex-forming oligonucleotides (TFOs). Existing TFOs have their limitations therefore there is a need to develop synthetic analogues that address this problem. This thesis describes a viable synthetic route for new pyridine-stretched nucleosides of diaminopurine (strD) and proposals for guanine (strG). These new bases are intended for incorporation into pyridine-stretched oligonucleotides (PSOs) for planned evaluation as potential new, antigene TFOs.

1'-Chloro-2'-deoxy-3',5'-di-*O*-toluoyl-α-D-*erythro*-pentofuranose **4**, which has proved to be a good reagent for the synthesis of 2'-deoxyribonucleosides, was synthesized in three steps from 2'-deoxyribose. Compound **4** was reacted with the cesium salt of 4(5)-nitroimidazole **5** giving four different isomers (**6-9**), which were identified by NMR. The glycosylation reaction was optimized by using the different solvents and different temperatures to maximize the yield of 1-(2′-Deoxy-3′,5′-di-*O*-toluoyl-α/β-D-*erythro*-pentofuranosyl)-5-nitroimidazole **6**. The nitro nucleoside **6** was hydrogenated with 5% Pd/C to give the amino derivative **10**, which was unstable on attempted isolation. To avoid the decomposition, amino derivative **10** was formed *in situ* and was reacted immediately on *C*-addition with ethoxymethylene malononitrile (EMMN) to give **11**. Despite repeated attempts this reaction was consistently low yielding. Cyclisation of **11** gave the pyridine ring and deprotection of the sugar in the same step gave **12** in high yield. Neutralization with citric acid was very important to maintain the product yield (84%). Finally, cyclisation of nucleoside **12** with guanidine gave strD. The highest yield (45%) was obtained using methanol at 145 °C in a steel bomb. The structures of all compounds were fully supported by their spectroscopic properties. Potentially viable routes to strG are proposed.

Keywords: 2'-deoxynucleosides, 5β-aminoimidazoles, DNA, *lin*-pyridoadenosine, nucleoside analogues

To Mum, Dad, Sister and my Sister's family

Acknowledgements

I would like to thank my supervisor Dr William Fraser for his expert guidance over last year.

Thanks for technical assistance go to Mr Mike L. Davis and Mrs Karen C. Farrow for their patient and kind advice and help.

Thanks for all my friends in medicinal chemistry department for their support.

A huge thanks to my parent and my sister for their financial support.

Content

Lists of Figures

List of Tables

Introduction

1.1 Background

The discoveries of the helical structure of DNA by Watson and Crick[1] and the recognition that DNA is the carrier of genetic information by Avery[2] have created a new field of science that brought chemistry and biology together, and led to the modern biology and biotechnology.

The recently emerging nucleic acid-based therapeutics (Figure 1) addressed regulation of gene expression *in vivo* by direct inhibition of mRNA through short complementary oligonucleotides (antisense and ribozyme strategies) or targeting oligonucleotides to the gene itself (antigene strategy)[3-6].

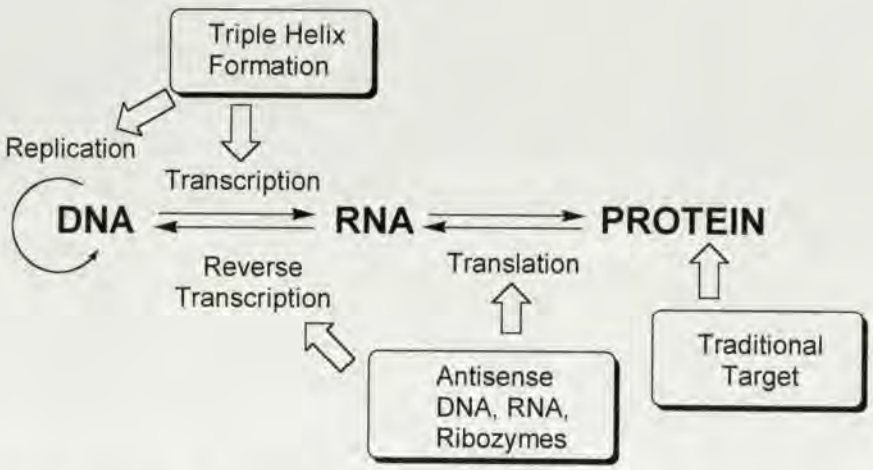

Figure 1. The central dogma of molecular biology and information transfer targets. The biological transfer and amplification of information from its stored form as double helical DNA to messenger RNA, and then to protein.

One way to recognize and inhibit the functioning of DNA or mRNA is through binding to a complementary base sequence. The antigene strategy exploits the possibility of binding exogenous nucleic acid analogues to the duplex DNA of the gene in order to hamper mRNA synthesis on the DNA

template while the antisense approach is directed against the functioning of the mRNA template for the synthesis of proteins. Because continuous gene expression keeps supplying new mRNA molecules, the antigene strategy to block the genes may be more efficient than the antisense approach as there is only one copy of the gene per cell compared with the many mRNA products. For either of these approaches to be effective, the antisense/antigene oligonucleotide must conform to all requirements of a functional drug such as cell permeability, stability in the cells and bioavailability at the desired target. In the antigene strategy discussed later (Section 1.4) much effort has been devoted to increasing the stability of triplexes under physiological conditions, such as conjugation of polyamines, triplex helix-specific intercalating agents, non-natural bases or the widely explored sugar-phosphate backbone modifications. A triplex is a three-stranded structure formed by duplex DNA in association with a third oligonucleotide; a triplex forming oligonucleotide (TFO). When purine or pyrimidine bases occupy the major groove of the DNA double helix they adopt Hoogsteen base pairing with the Watson-Crick base-paired target duplex. A variety of chemically modified TFO analogues are being designed, synthesized and evaluated to meet the requirements of effective triplex formation. As research has carried on, with Hélène and Devan's discoveries[7,8], the interests on non-natural base modifications are growing. Several research groups[9-13] have shown that changing the natural bases (Figure 2) for non-natural bases could significantly improve the triplex stability of TFOs under physiological conditions.

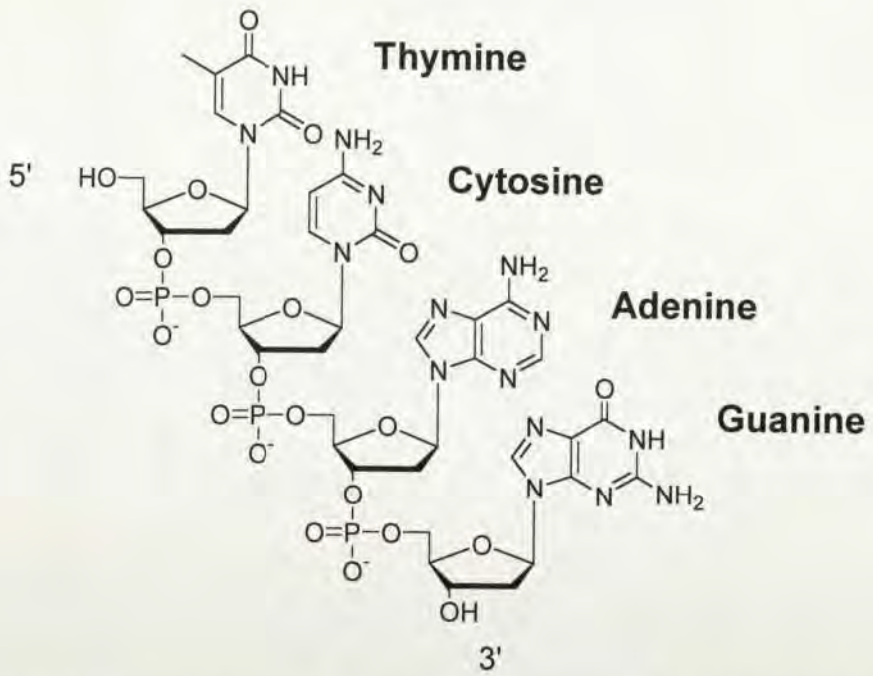

Figure 2. DNA consists of a chain of 2'-deoxy-D-ribose units linked by 3'-5' phosphodiester moieties, each carrying one of the possible heterocyclic bases in a β-configuration at the C1' sugar position. The four different natural bases: G, A, C and T are show above.

This report describes a viable synthetic route for new pyridine-stretched nucleosides of diaminopurine (strD) and guanine (strG). These new bases are intended for incorporation into pyridine-stretched oligonucleotides (PSOs) for planned evaluation as potential new, antigene TFOs.

Antisense and ribozyme approaches are described in this report to set the context for the antigene strategy. Compared with the antigene strategy, antisense and ribozyme strategies, which also have possible roles in future gene therapy, are relatively well-developed strategies that have been widely studied. More and more observations from antisense and ribozyme studies have been used to develop the antigene strategy further. The fascinating the history and developments in these areas are worth exploring.

1.2 Antisense Strategy (RNA Strategy)

Any single-stranded DNA or RNA that possesses the ability to block the transfer of information from the genetic template to expressed protein by interfering with the expression of mRNA is called an antisense oligonucleotide (ASO). This process occurs naturally and allows the complementary pairing of antisense nucleic acid strands to regulate and balance various genes. Zamecnik and co-workers in 1978[14,15] demonstrated the first use of an oligonucleotide to target RNA in a sequence-dependent manner and, therefore specifically inhibit synthesis of the chosen target protein. Subsequently, several synthetic oligonucleotides have reached clinical trials for a variety of indications, including leukaemia, cancer and AIDS[16]. The Food and Drug Administration has approved use of first antisense oligonucleotide fomivirsen, against ganciclovir-resistant cytomegalovirus.

1.2.1 Chemical Structure and Biology of the RNA Strategy

Naturally occurring antisense RNAs are small, diffusible, highly structured RNAs that act, via sequence complementary, on target RNAs called sense RNAs. In eukaryotes, some processes like splicing or editing also make use of complementary small RNAs, although these RNAs are not independent regulators[17]. In the classical case, antisense RNAs are encoded in cis. They are transcribed from a promoter located on the opposite strand of the same DNA molecule, and are, therefore, fully complementary to their target RNAs. However, a number of antisense RNAs that are encoded in trans, were

detected and reveal only partial complementarities to their target RNA which can be more than one. The sense RNAs are mostly mRNAs encoding proteins having important or essential functions. In the majority of cases, antisense-RNA action entails post-transcriptional inhibition of target RNA function. Naturally occurring antisense RNAs are between 35 and 150 nucleotides (nt) long and comprise between one and four stem-loops. They are sensitive to extracellular fluid nucleases. Efficient antisense RNAs have 5–8 nt GC-rich loops. Phosphodiesters undergo bulk internalisation predominantly from pinocytosis (fluid-phase endocytosis) when transported intracellularly. Bulges (if >10 bp) often interrupted the phosphate backbones to prevent double stranded ribonuclease (dsRNase) degradation and to facilitate melting upon antisense/sense RNA interaction[18,19], although they are also important for metabolic stability.

1.2.2 ASOs: Mechanism of Action

Several proposed theories have been used for the mechanism of action of ASOs (Figure 3). The first theory involves direct binding of the ASO to its mRNA target through standard Watson-Crick base-pairing. The formation of double-stranded structures is based on the presence of hydrogen bond donors and acceptors in the nucleobases. Figure 4 shows two complementary base pairs of double-stranded DNA. Gene expression is thereby prevented by the ASO because of steric blocking of the ribosomal machinery[20-22]. Other theories implicate that in order to achieve hybrid-arrest translation, the ASO strand should cover part of the RNA extending from the 5'-capping site to

about 15 nucleotides downstream of the initiation AUG codon[21,23,24]. However, once fully assembled, the ribosome has the ability to "melt out" any ASO/RNA complexes formed along the mRNA, which means that steric blocking can prevent only the initiation step of translation. The fact that target mRNA do not always remain intact during this process suggests that ASOs can induce the degradation of the RNA part of the ASO/RNA hybrid by the enzyme ribonuclease H (RNase H)[25,26]. RNase H is an endogenous enzyme, which is located within the nucleus and is involved in DNA replication[27-29]. ASO-mediated RNase H degradation of the target mRNA can occur at any stage of gene expression: splicing, translation or reverse transcription.

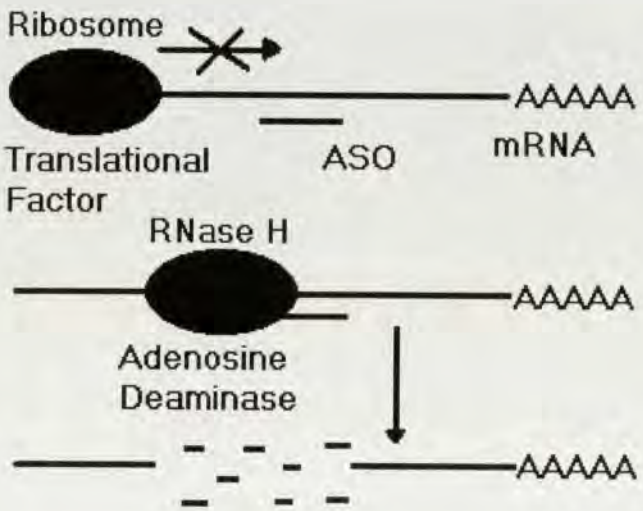

Figure 3. ASO mechanism of action. Once the ASO is targeted to mRNA, activation of RNase H leads to the degradation of the duplex antisense mRNA. Since the mRNA is eliminated, no protein can be formed, leading to a phenotypic change. Adenosine deaminase is also implicated in the degradation of the antisense/mRNA duplex[30].

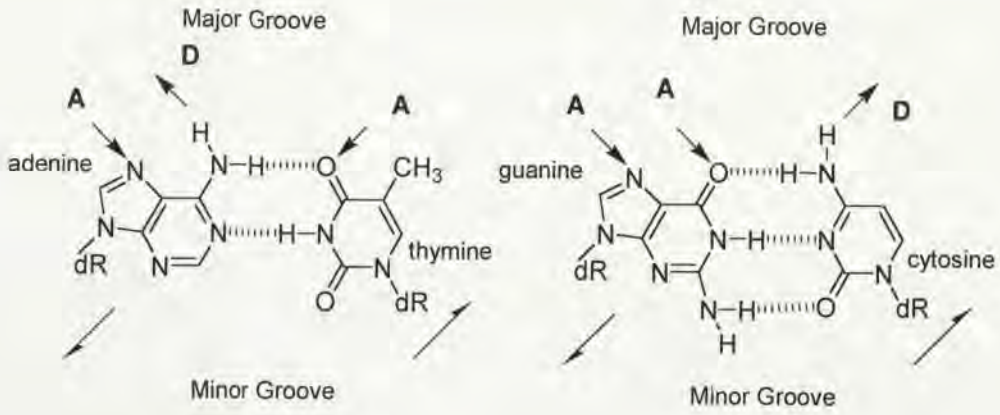

Figure 4. Hydrogen bond formation between complementary bases leaves several H-bonding sites, indicated by full headed arrows (donor, **D** or acceptor, **A**), vacant in the major groove of the duplex. Adenine and guanine (purines) have distinct bidenate sites vacant whereas cytosine and thymine (pyrimidines) have only a single available binding site in the major groove. Half-arrows indicate the relative deoxyribose-phosphate (dR) backbone orientation.

1.2.3 Limitations of the Antisense strategy

Antisense therapy faces several limitations. The most concerning of these limitations are the nonantisense mechanisms of action that cause confusion in the interpretation of results[20]. Antisense approaches suffer removal of bases, deamination/depurination, which occur during metabolic degradation in plasma[31-33]. Therefore, in order to reach maximal therapeutic affect, high concentrations of ASOs are used but with the drawback of doses limiting toxicity and immunostimulatory effects[34,35]. Chemical modifications can show advantages, if they could possess suitable pharmacokinetics, which would allow specific delivery to the targeted tissue in non-toxic and cost-effective doses.

1.3 Ribozymes

Ribozymes are small RNA molecules capable of catalytic activity. Tom Cech first discovered ribozymes, or catalytic RNAs[36,37], which were characterized originally within the Group I intervening sequence of pre-rRNA of *Tetrahymena thermophila*. This sequence catalyses its own excision, and has been termed self-splicing. The RNA portion of the RNase H enzyme purified from *E. coli* was the first reported truly catalytic ribozyme[38]. Other studies have shown that the plus strand of tobacco ring spot virus possesses a hammerhead shape and the minus strand exhibits a hairpin shape[39]. The widespread existence in nature makes ribozymes highly possible candidates for future gene therapy. Recently research has found that the RNA components of some, perhaps many ribonucleoprotein complexes, may have catalytic activity; such may include the highly deproteinized ribosomes that can catalyse peptide transfer[40,41]. Initially, ribozymes were thought to act only in cis conformation for cleavage reactions, but the hammerhead ribozyme has been found to act in trans[42], as well as the hairpin ribozyme[43].

1.3.1 Chemical Structure and Biology of Ribozymes

Up to now, six types of RNA motifs have been identified: Group I introns, RNase P, hammerhead ribozymes, hairpin ribozymes, axehead ribozymes of the hepatitis delta virus (HDV), and RNA transcripts of the mitochondrial DNA plasmid of Neurospora[44,45]. These ribozymes are broadly separated into two classes based on their size and reaction mechanisms[46]. The large ribozymes consist of RNase P, and the group I and group II introns. These

molecules range in size from a few hundred nucleotides to around 3000. These catalyse reactions that generate reaction intermediates and products with 3' hydroxyl and 5' phosphate groups. The small ribozymes include the hammerhead, the hairpin (or paperclip) and hepatitis delta. These molecules range in size from ~35 to ~155 nucleotides. They use the 2' hydroxyl of the ribose sugar as nucleophile, and they generate products with a 2',3'-cyclic phosphate and a free 5' hydroxyl group. The reaction mechanism and the size of the large ribozymes are needed to bring often very distal elements of the substrate into close proximity; the small, self-cleaving, RNAs are faced with this constraint and perhaps this permitted them to evolve smaller catalytic centres. It remains possible, however, that the relationship between the size and reaction mechanism is simply fortuitous.

1.3.2 Ribozymes: Mechanism of Action

There are two-postulated mechanisms for the activity of ribozymes: (1) steric blocking, where the binding of substrate to the mRNA prevents any further translation or metabolism of the RNA molecule; (2) cleavage and inactivation of the targeted mRNA. Formerly, ribozymes were observed to generally catalyse intramolecular, single-turnover reactions in nature. Recently, an exhaustive comparison of the enzymatic mechanisms of protein and RNA enzymes has been made[47]. Ribozymes demonstrate the capacity for multiple turnovers; one ribozyme molecule may inactivate multiple RNA molecules (Figure 5).

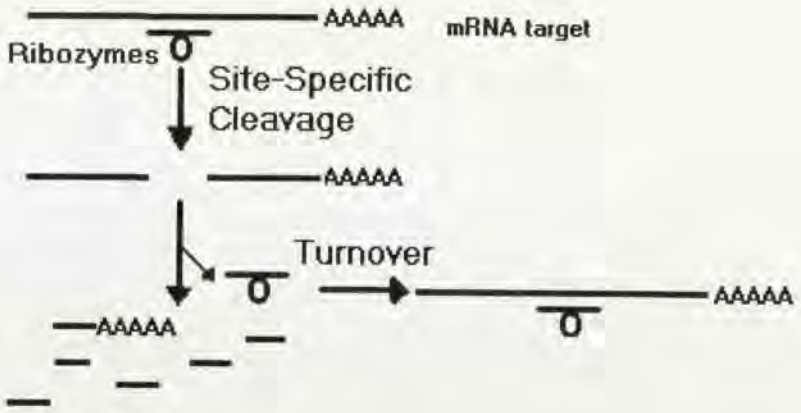

Figure 5. Mechanism of ribozyme action. Ribozymes are capable of multiple turnovers. Once the ribozyme cuts its target mRNA, it is able to dissociate from the target and cleave a second mRNA. The cleaved mRNA is though to be inactivated and then degraded by unspecific nucleases, leading to suppression of mRNA translation and protein production.

All known ribozymes have an absolute requirement for a divalent cation, which is generally Mg^{2+}. Notable within the large catalytic RNAs, are some that require divalent cations for proper assembly of the tertiary structures as well. On this basis, catalytic RNAs are considered metalloenzymes, and a general two-metal-ion reaction mechanism has been proposed for the large catalytic RNAs, based on analogy with the properties of protein metalloenzymes[48]. The role of divalent cations for the small catalytic RNAs is less clear, but they are generally considered to be essential for catalysis[49].

1.4 Antigene Strategy (DNA Strategy): Triplex Forming Oligonucleotides (TFOs)

It was only four years after the discovery of the double helix that a publication by Felsenfeld, David and Rich described the formation of a triple helix involving one poly A and two poly U chains[50,51]. In order to be selective for a unique DNA sequence within the human genome of 3×10^9 base pairs, such Triplex Forming Oligonucleotides (TFOs) need to recognize at least 16 or 17 consecutive bases. Sequence-specific contacts with the regular array of hydrogen bond donors and acceptors on the base pairs, which are exposed in the major and minor grooves, is a necessity (Figure 4). Duplex DNA is able to bind to TFOs to form triple-stranded structures containing one polypurine and two-polypyrimidine strands[52-54]. Research on the multi-stranded structure of polynucleotides is based on these discoveries. However, in the early days, the limited information available at that time restricted further developments, as only homopolynucleotides and alternating polynucleotides were known. The interest in triple-helical structures then decreased due to the lack of diversity in the sequences that could be investigated and the absence of a demonstration of biological function for such structures. In the 1980s, interest in TFOs arose after the following two major developments:

- Homopurine-homopymidine stretches in supercoiled plasmids were found to adopt an unusual DNA structure call H-DNA (these include a triplex as the major structural element[55,56]);
- Several groups demonstrated that homopyrimidine and some purine-rich oligonucleotides can form stable and sequence-specific complexes with corresponding homopurine-homopyrimidine sites of

duplex DNA[7,57,58]. These complexes were found to be triplex structures rather than D-loops, where the oligonucleotide invades the double helix and displaces one strand. A characteristic feature of these triplexes is that the two chemically homologous strands (both pyrimidine and purine) are antiparallel (Figure 6).

These findings led to an increased interest in triplex studies.

1.4.1 Chemical Structure and Biology of TFOs

Two main classes of triple helix have been characterized, which differ according to the orientation and base composition of the third strand. Pyrimidine-rich third strands bind parallel to the duplex purine strand and include T*A.T and C^{+}*G.C triplets (Figure 6) (Py*Pu.Py). Purine-rich oligonucleotides bind in antiparallel orientation and include G*G.C, A*A.T triplets (Figure 6) (Pu*Pu.Py). In Figure 6, where Py = pyrimidine, Pu = purine, * = Hoogsteen hydrogen bonds, and the full stop = Watson-Crick base-pairing. The third strand may be composed of RNA or DNA chains or their combination. Many studies have shown that triplex structures vary greatly depending on the exact conditions that include pH and salt concentration[59]. Recently research showed that the orientation of TFOs might follow other additional principles. For example, G and T containing TFOs can bind in either orientation; parallel or antiparallel[59] (Figure 6).

To form the colinear association of three oligodeoxynucleotide strands, the third strand binds with the purine strand of the Watson-Crick base pairs by Hoogsten hydrogen bonds within the major groove of the DNA double helix. Intramolecular triplexes may form when a part of the DNA double helix folds

back upon itself in homopurine-homopyrimidine regions of supercoiled DNA[60,61].

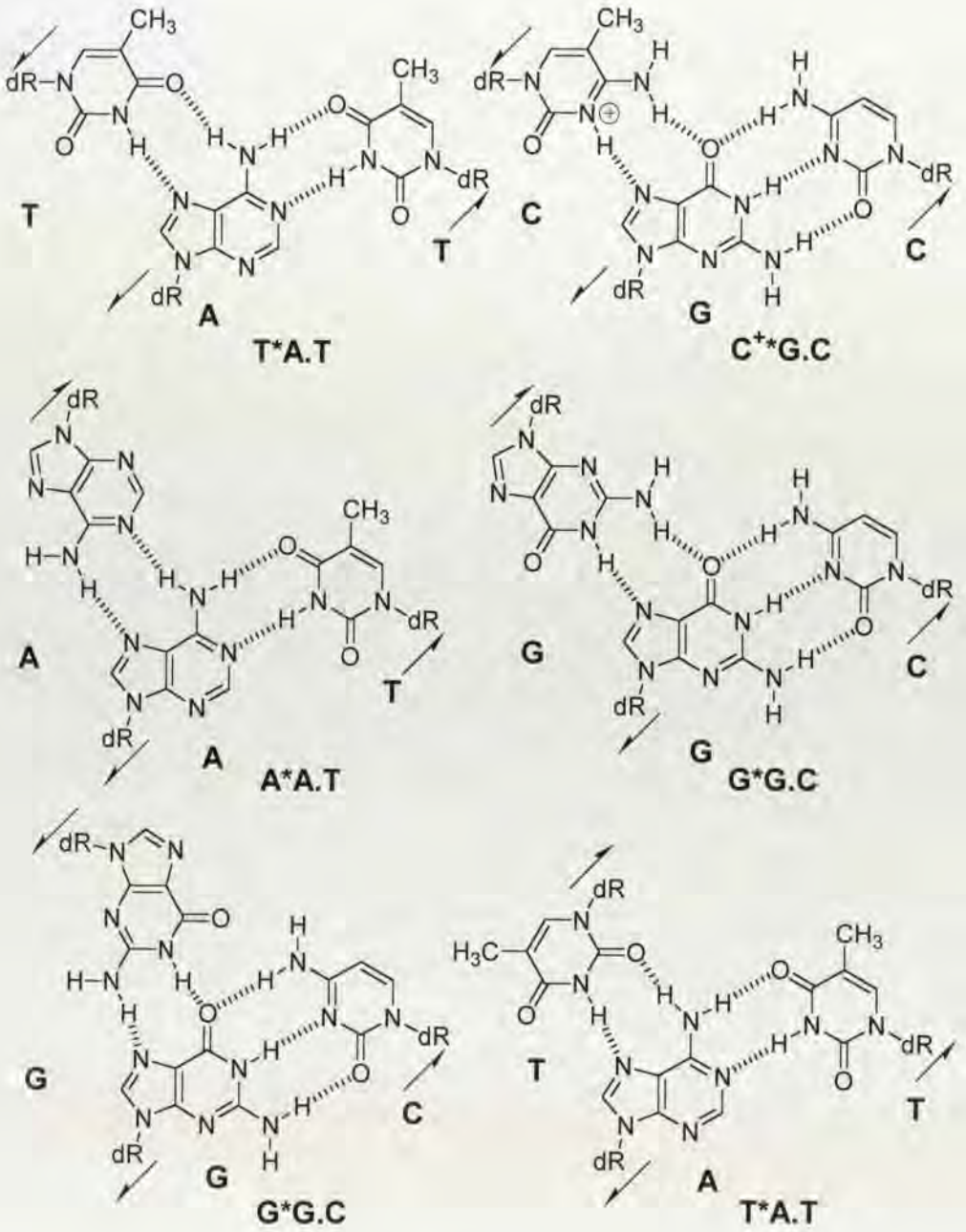

Figure 6. Structures of the parallel triplets C^{+}*G.C, T*A.T and G*G.C. and antiparallel triplets A*A.T, G*G.C and T*A.T. Half-arrows indicate the relative deoxyribose-phosphate (dR) backbone orientation.

N3 protonation of cytosine in the third strand is crucial to formation of the C^+G^*C triad and maintain the second hydrogen bond of the Hoogsteen pair. The pK_a of the free cytosine is about 4.5, this is elevated on triplex formation and may be as high as 6.5 for an isolated internal cytosine. At pH 6.5 and below, C^+ can form 2 Hoogsteen hydrogen bonds with its target G.C base pair. But at pH 7.2 and above, C is unprotonated meaning loss of the N3-H-N7 hydrogen bond to G causing further triplex destabilization. Several cytosine analogues have therefore been designed with the aim of forming pH-independent Hoogsteen hydrogen bonds with guanine (Section 1.6.1.1).

For the antiparallel DNA triplexes, most of them are Pu*Pu.Py. A recent study has shown that the Py*Pu.Py triplet, can also adopt the antiparallel structure with reversed Hoogsteen hydrogen bonds (Figure 6). Compared with the parallel DNA triplexes containing C^+ and T, which require of low pH values, the purine-containing TFOs are stable over a wider pH range. However, the studies on the stability of antiparallel triplexes found that their triplex stability varies widely and depends on sequence. In some studies short oligonucleotides exhibit nanomolar binding constants[62,63] while in other studies longer oligonucleotides, under similar conditions, fail to show binding at micromolar concentrations[64-67]. This may be due to the different relative positions of the third strand TFO backbone in G*G.C, A*A.T and T*A.T triplets compared to the parallel T*A.T and C^+*G.C triplets, which are isohelical (Figure 6). Furthermore, the observation that the affinity of antiparallel triplets is dominated by the G*G.C triplets, which imparts a much greater stability than either A*A.T or T*A.T[64]. However, G-rich oligonucleotides form strong inter- and intramolecular structures, possibly

involving G-quartet formation, which reduces the effective concentration of the oligonucleotide by competing with triplet formation. The best antiparallel triplexes may therefore be those in which the third strand has a high G-content, but in which the guanines are arranged in such a way as to prevent the formation of unusual structures; low numbers of contiguous G bases for example.

1.4.2 TFOs: Mechanism of Action

Figure 7 shows the principle of action of TFOs in their binding to a particular gene to prevent expression and normal function. The TFO binds to the purine-rich strand of DNA via Hoogsteen hydrogen bonds between the third-strand nucleotide and its complement in the purine-rich strand. The third strand of the TFO may contain either polypurines or polypyrimidines. Thermal studies have identified that the most stable combinations for polypurine third strands are G*G.C at neutral pH[61]. Though purine TFOs bind well at physiological pH, physiological K^+ concentration can inhibit binding, particularly in G-rich TFOs[68]. These triplexes are also dependent on the presence of multivalent cations such as Mg^{2+}, which mediates charge neutralization when the three anionic phosphodiester backbones come together. The optimal triplet combinations in a polypyrimidine third strand are T*A.T and C^+*G.C, although the formation of C^+*G.C Hoogsteen bonds require an acidic pH for optimal stability.

The specificity of triplex formation is the direct result of the formation of complementary Hoogsteen base pairs between the purine-rich strand of the

target DNA and the TFO. DNase I protection and electrophoresis mobility shift assays have shown that TFOs have the ability to discriminate to one base triplet[69]. After TFO binding, the physical presence of a third strand, as well as the conformational change of the helical structure, prevents the DNA/protein interactions necessary for efficient transcription[70,71].

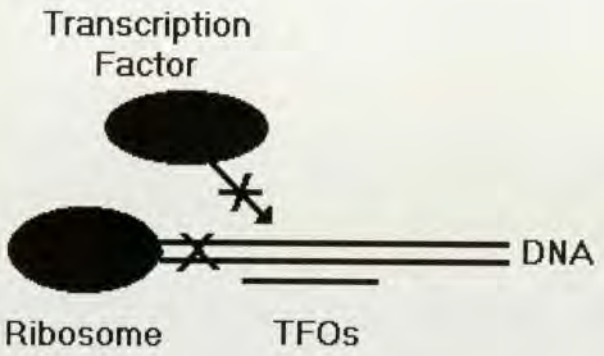

Figure 7. Mechanism of TFOs. TFOs perturb gene expression by associating with a specific region of a promoter to alter the transcription of the regulated gene[30].

1.4.3 Limitations of TFOs

Triplex formation is limited by the following drawbacks. The requirement for oligopurine tracts on the target DNA. This limitation arises from the recognition mechanism, which involves the purine's two remaining Hoogsteen hydrogen-bonding sites in the major groove for he DNA duplex. Pyrimidines have only one hydrogen-bonding site available and cannot bind as strongly as purines. The pH dependence of C-containing TFOs means that there are unstable at physiological pH since protonation of cytosine to give C^+ in acidic media is necessary to maintain the integrity of the Hoogsteen pair. Antiparallel triplexes containing G, A and T can form at the physiological pH.

However, base triplets containing G*G.C, A*A.T or T*A.T are not isomorphous meaning location and orientation of the third strand is sequence dependent. This leads to helix distortion for mixed sequences especially in the case of G*G.C and T*A.T sequences.

1.5 Benefits and Drawbacks of the Different Strategies

The antigene strategy targets oligonucleotides to genes themselves and presents several advantages compared with antisense oligonucleotides or ribozymes that are directed to messenger RNAs.

There are only two copies (two alleles) of the targeted gene whereas there may be thousands of copies of a messenger RNA, and the antisense and ribozymes oligonucleotides must be present in excess numbers when compared with the target in order to completely ablate the gene function. Blocking mRNA translation even by inducing sequence-targeted cleavage of the RNA chain does not prevent the corresponding gene from being transcribed, thereby repopulating the RNA pool. In contrast, preventing gene transcription is expected to lower the mRNA concentration in a more efficient and lasting way, depending on residence time of the antigene oligonucleotide on its target sequence and its lifetime determined by its nuclease sensitivity and susceptibility to hydrolysis. Triplex-forming oligonucleotides act at the transcription level inhibiting the synthesis of the pre-messenger RNA. All RNA species arising from alternative splicing reactions are no longer synthesized. Inhibiting mRNA translation through a physical mechanism or an RNase H-dependent process does not arrest transcription and therefore the

mRNA pool is continuously repopulated. Therefore, either the antisense oligonucleotide should have a catalytic mode of action or should be present at a sufficient concentration for a long enough period of time to obtain a permanent down-regulation of protein synthesis. Of course there might be cases where a transient inhibition of gene expression may induce an irreversible process so that the biological response no longer requires the action of the antisense oligonucleotide. A permanent inhibition of transcription requires that either the oligonucleotide induces an irreversible reaction or the oligonucleotide-DNA triple helical complex survives for a long enough time. Ribozymes should have advantages over antisense oligonucleotides due to their capacity for multiple turnover reactions with their target, as demonstrated *in vitro*. At the moment, no clinical trial data is available on ribozyme therapeutics that demonstrates this potential *in vivo*. As a consequence, the oligonucleotides for the antigene strategy, such as peptidic nucleic acids (PNAs) (Figure 14e) and TFOs, will have an impact for future treatment of diseases and delineating the function of new genes at the cellular level.

1.6 Improving the TFO Strategy

TFOs bind with high specificity, however, this is limited by the stability of triple-helical complexes formed with natural third strands, which is generally weak, except for the few containing G-rich purine sequences. Binding of TFOs may not be as strong as that of the targeted DNA duplex itself. This is thought to be largely due to charge repulsion resulting from bringing together the three polyanionic DNA strands. Moreover, *in vivo* applications require

TFOs to form not only triple-helix structures under physiological conditions but also to reach their targets before being degraded by cellular nucleases. Concerning nuclease resistance, TFOs have benefited from improvements made to the antisense oligonucleotides. Numerous investigations on TFO analogues involving base, sugar or backbone modifications or attachment of intercalating agents have been carried out in order to improve the potential of oligonucleotide-directed triple-helix formation (Figure 8). Several approaches have been used and are discussed in the following sections.

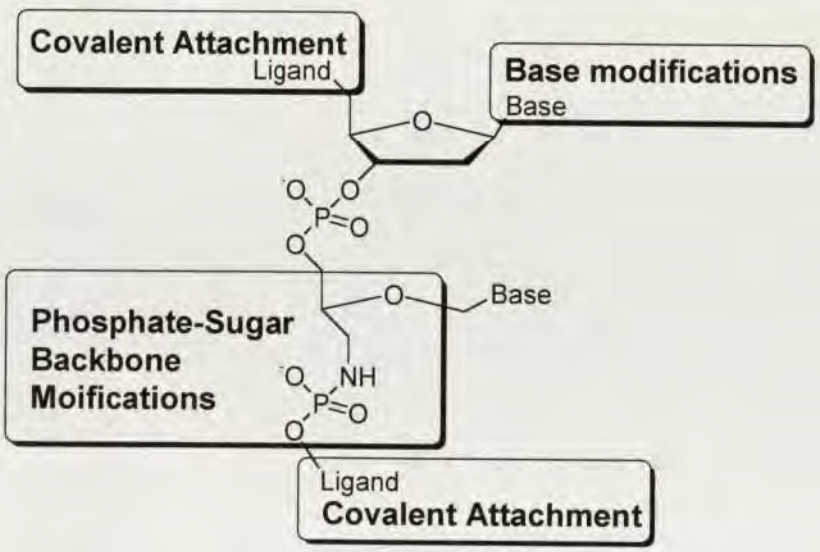

Figure 8. Potential sites for oligonucleotide modifications to generate triplexes with enhanced stability.

1.6.1 Base Modifications

1.6.1.1 Py*Pu.Py triplexes

For TFOs containing C, one limitation to the formation of stable triplexes is pH dependence as formation of a C^+*G.C triplet that requires protonation of the third strand cytidine residues at N3 in order to form two Hoogsteen hydrogen bonds (Figure 6). The first solution to provide more stable Py*Pu.Py triplexes at physiological pH was replacement of cytidine by 5-methycytidine[72,73] (Figure 9a). This modification enhanced considerably the stability of helices at neutral pH. However, the influence of cytidine methylation on triplex stability does not appear to result from the 0.2 unit pK_a increase. It is mainly of entropic origin[74]. A plausible explanation of this effect is that the methyl group should fill a space in the major groove of the targeted DNA duplex, causing a release of hydrating water molecules from the double helix; a source of positive entropy change. Recently numerous synthetic nucleosides have been developed that display the hydrogen-bonding pattern of protonated cytidine (Figure 9). These synthetic cytidine analogues are able to form two hydrogen bonds with G of the G.C base pair, without protonation, or are able to undergo protonation under physiological conditions. Among the neutral nucleosides reported, 5-methyl-6-oxocytidine[75] (Figure 9b), pseudoisocytidine[76] (Figure 9c), 6-oxocytosine[75,77] (Figure 9d), and pyrazine analogue[78] (Figure 9e) have proven efficient for targeting G.C stretches. These heterocycles already have a hydrogen atom at the N3 position, which allows them to bind to G in a pH-independent fashion. Triplexes containing these modified bases are more stable at neutral pH than

cytidine-containing triplexes but generally do not achieve the stability of 5-methylcytidine-containing triple helices. Thus the triple to double helix transition temperatures (T_m) of triplexes containing $m^{5ox}C$ is still significantly lower at neutral pH than those observed for the corresponding m^5C^+-containing triplexes. One exception, among the cytidine surrogates protonated at physiological pH, the recently reported 2-aminopyridine[79,80] (Figure 9f), which exhibited interesting properties. Between a 6-8 pH range, TFOs containing this cytidine analogue bind strongly to and with increased specificity for their duplex target, compared with those containing 5-methyl-2'-deoxycytidine[81]. Furthermore, 2-aminopyridine-containing pyrimidine TFOs are able to bind with targets containing stretches of G.C at physiological pH, whereas those containing 5-methyl-2'-deoxycytidine are not.

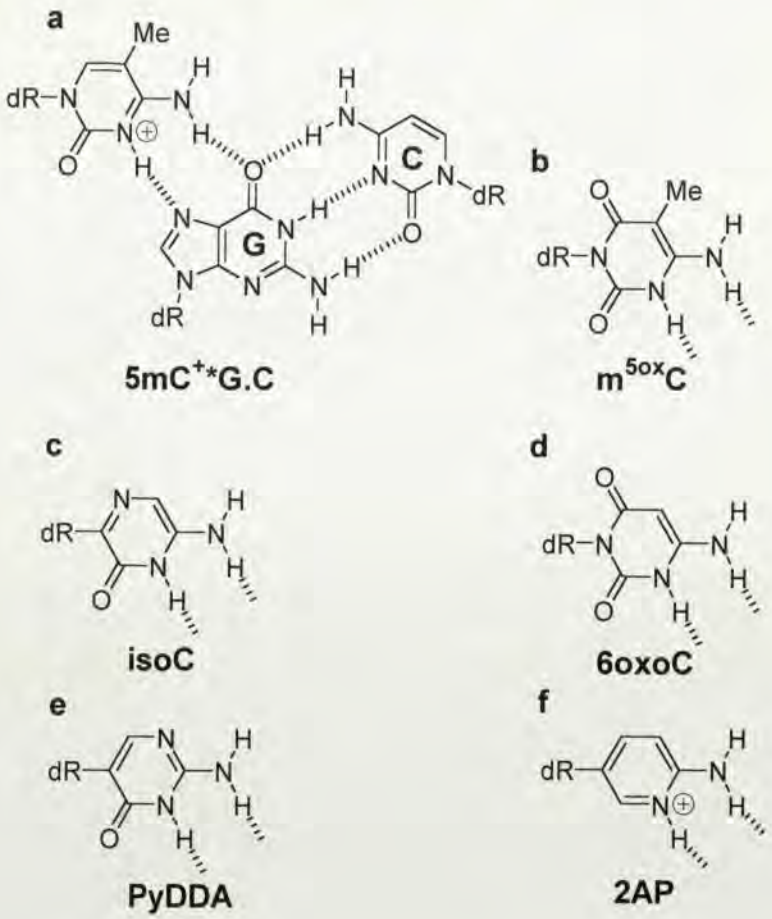

Figure 9. Cytidine analogues for recognition of G.C base pairs in a parallel triplex. **a**) The $5mC^{+}$*G.C triplet, **b**) 5-Methyl-6-oxocytidine, **c**) Peseudoisocytosine, **d**) 6-Oxocytosine, **e**) Pyrazine analogue, **f**) 2-Aminopyridine. In **b** - **f** the third strand base analogue is shown alone in the same orientation as in **a**, indicating the substituents that form hydrogen bonds with G.

1.6.1.2 Purine-Like Cytidine Base Analogues

Some purine-like cytidine bases have been described for improvement of the pH dependence shown by the natural cytidine (Figure 10). They include 3-methyl-5-amino-1*H*-pyrazolo[4,3-*d*]pyrimidine-7-one[82-84] (P1) and its positional isomer P2. In these structures deoxyribose is linked to the pyrazole N^2 for P2 and to N^1 for P1. N^6-Methyl-8-oxoadenosine[85] (^{8ox}A) and N^7-guanosine[84] (^{7}G) have also been reported (Figure 10). However, these

analogues are not isostructural with T*A.T as the sugar-phosphate backbones (dR) are in different relative positions.

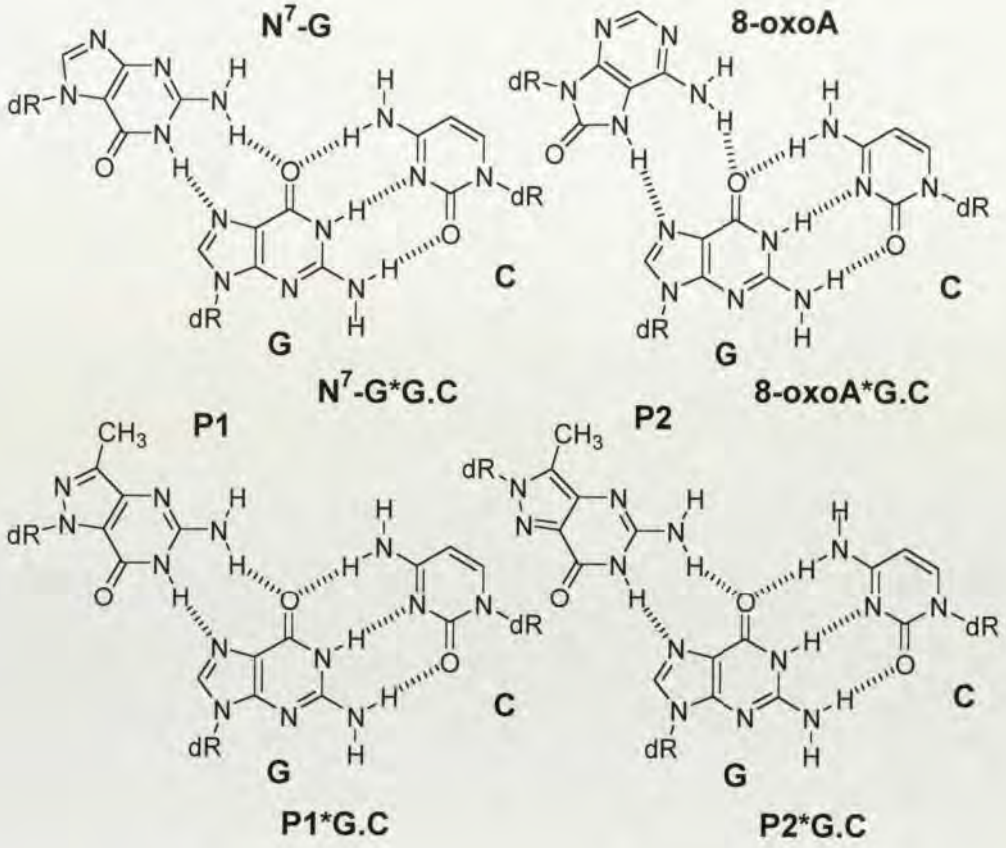

Figure 10. Structures of purine-like cytidine mimics for recognition of G.C base pairs in a parallel triplex.

1.6.1.3 Targeting to Py.Pu Duplexes

The requirement for the oligopurine tracts on the target DNA also restricts the available targets DNA for the antigene strategy. The limitation arises from the recognition mechanism, which involves the purine's two remaining Hoogsteen hydrogen-bonding sites in the major groove of the DNA duplex (Figure 4). Pyrimidines have only one hydrogen-bonding site vacant and cannot efficiently bind. Therefore, several non-canonical natural base triplets

of intermediate stability, such as G*T.A in a Py*Pu.Py context and T*C.G were discovered following a systematic study[59]. Both base triplets involve a single hydrogen bond between the third-strand base (G or T) and the target pyrimidine inversion (T or C) (Figure 11). However, these solutions have limited destabilization rather than active improvements to pyrimidine recognition. For this reason, an alternative solution would be to bind the facing purine of the opposite strand instead. Along these lines, formycin A (^{for}A) was observed to form two hydrogen bonds with the guanosine of the other strand at C-G inversions in a Pu*Pu.Py triplex[86], as shown in Figure 12. To do so however, a 3 to 5 Å translation as well as a rotation around the ribose-phosphate backbone is required, which would result in severe backbone distortion. Incorporation of three ^{for}A*C.G instead of G*C.G resulted in a ten-fold increase in binding affinity[86], but this may also coincidentally be due to reduced steric hindrance of formycin relative to guanine.

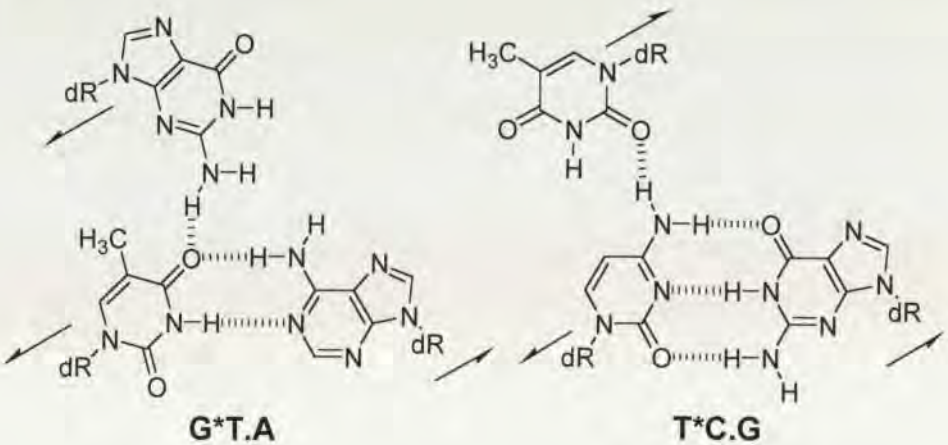

Figure 11. Non-canonical G*T.A and T*C.G base triplets in a Pu*Py.Pu or Py*Py.Pu context. In contrast to the canonical purine recognition scheme, only a single hydrogen bond can be drawn between third strand and target bases.

Indeed, when comparing ^{for}A*C.G and G*C.G triplets within the Pu*Pu.Py backbone geometry (Figure 12), formycin escapes the G(N^1-H and N^2-H)/C(N^4-H) clash and may even take advantage of an attractive ^{for}A(N^1)/C(N^4-H) interaction. The future success of this approach will rely on the possibility of crossing the DNA duplex major groove with more extended structures and without backbone distortion.

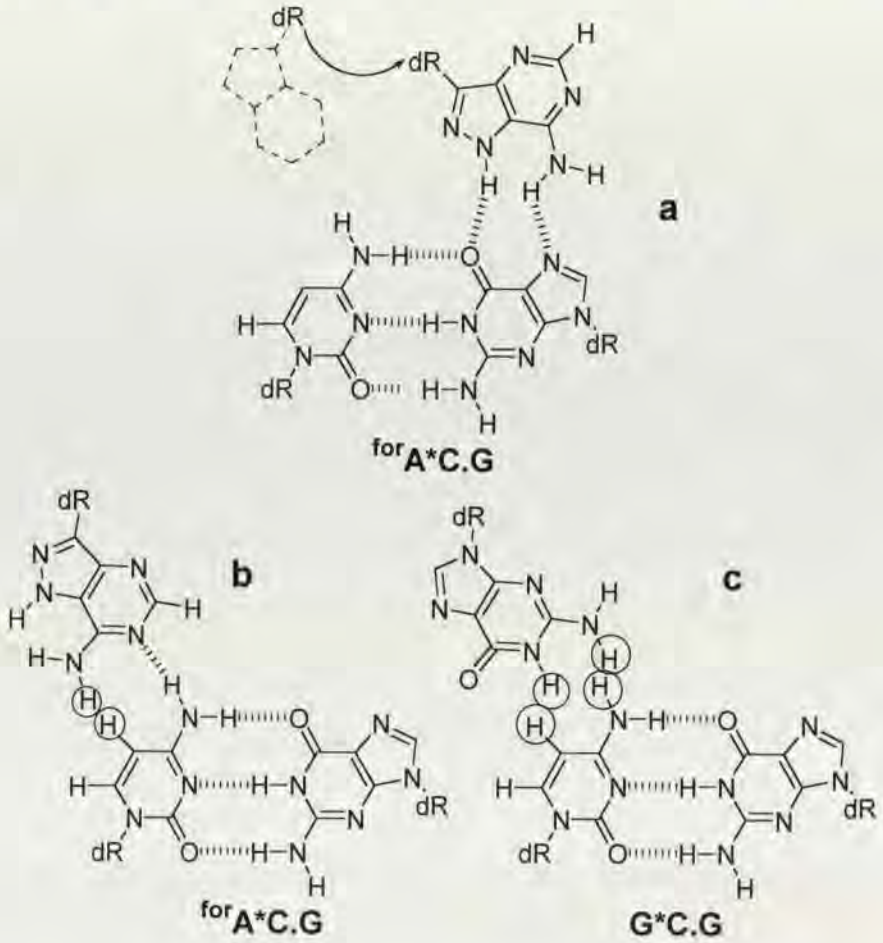

Figure 12. (**a**) For cytosine recognition, ^{for}A could hydrogen bond to guanine of the opposite DNA strand at the expense of a *ca.* 5 Å translation (arrow) through the major groove. The dotted line structure indicates the position of guanine in a G*G.C triplex. (**b**) ^{for}A, and (**c**) G facing the same C.G inversion.

1.6.1.4 Pu*Pu.Py triplexes

Compared with pyrimidine-containing oligonucleotides, which require conditions of low pH, the purine-containing oligonucleotides show obvious advantages in their pH independence. Nonetheless, non-isomorphism in structure and the formation of self-associated structures (G tetrads) restrict their wide spread use. In order to overcome the problem of non-isomorphism in the case of T*A.T/G*G.C triplexes, purine analogues of thymidine have been incorporated in third strand oligonucleotides. 7-Deaza-2'-deoxyxanthosine[87] (dzaX) and 2-aminopurine[88] (amP) has been used instead of T (or A) for A.T base pair recognition (Figure 13). Those involving 7-deaza-2'-deoxyxanthosine and 2'-deoxyguanine or 2-aminopurine and 2'-deoxyguanosine were shown to strongly hybridise with the target sequence, under physiological conditions, whereas the oligonucleotides containing 2'-deoxyguanosine and thymidine did not bind. To try to overcome the problem of self-association, several analogues of guanine have also been incorporated into TFOs. Such examples are 7-deazaguanine[87] (^{7}dzaG) and 9-deazaguanine[89] (^{9}dzaG), which are intended to disrupt the H-bonding network of the G-tetrad, whilst retaining the hydrogen bond donor-acceptor pattern for formation of dzaG*G.C triplets.

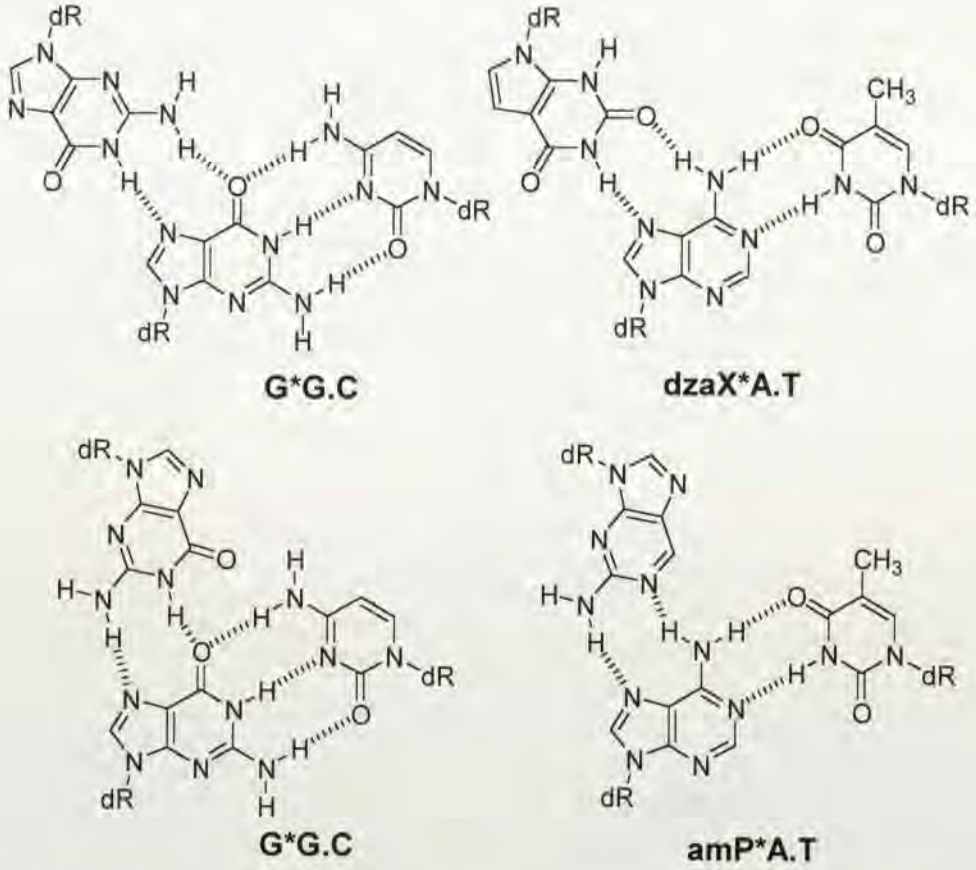

Figure 13. 7-Deazaxanthosine (dzaX) and 2-aminopurine (amP) could form isomorphous base triplets with A.T in a G*G.C context, by reverse-Hoogsteen bonding for dzaX or Hoogsteen bonding for amP.

1.6.2 Modification of the Sugar-Phosphate Backbone

Backbone modification is one of the developing approaches to optimise triplex stability, to maintain sequence specificity, to minimize self-associations, and furthermore to produce oligonucleotides that are resistant towards degradation by cellular nucleases. For this purpose, several families of derivatives were investigated, such as replacement of non-bridging atoms as in the case of phosphorothioate[90] (Figure 14b), bridging atoms as in the case of N3'→P5' phosphoramidates[91] (Figure 14c) or methyl phosphonate[12] (Figure 14d). In the case of peptide nucleic acids[92] (PNAs) (Figure 14e) a

more significant change is made in that the sugar-phosphate backbone (Figure 14a) is replaced by a polyamide backbone.

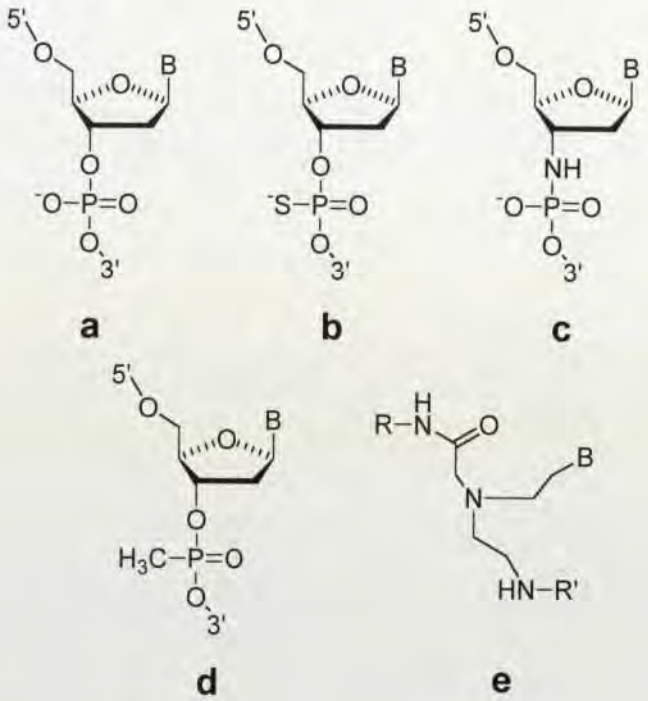

Figure 14. Different backbone modifications conferring stability towards intracellular nucleases and used in the antigene strategy. **a**: Phosphodiester, **b**: Phosphorothioate, **c**: N3'→ P5' phosphoramidate, **d**: Methyl phosphonate, **e**: Peptide Nucleic Acid (PNA).

Phosphorothioate (PS) modification confers resistance to nuclease degradation, and the hybrid formed with RNA is still recognized and cleaved by RNase H, which makes it extensively used in the antisense strategy. This modification was originally introduced into oligonucleotides in order to protect their quite labile internucleoside phosphodiester linkages against hydrolysis by extra- and intracellular nucleases[93]. Substitution of phosphorothioate linkages for the phosphodiester counterparts leads to creation of a new stereocenter at each modified internucleoside phosphorus

atom and, as anticipated, significantly protects oligonucleotides against enzymatic degradation[94]. Formation of triple-stranded complexes by the oligonucleotide phosphorothioates as a third strand binding to phosphodiester duplexes has also been extensively studied. When stereorandom or stereopure phosphorothioate linkages are incorporated into the purine-containing TFOs, stable triplexation is supported with the third strand running either antiparallel or parallel to the duplex targets[95,96]. Cell culture experiments indicated that the triplex stability of the (PS) derivatives with the (G,A)[97-100] or the (G,T)-motif[101], is similar to their phosphodiester (PO) analogues. However, triplex stability is greatly reduced in the pyrimidine motif by this modification[97,102,103].

Methyl phosphonate (MP) with its neutral backbone, and in the purine motif, binds to a duplex or a single-stranded nucleic targets forming duplex and triplex structures. This modification was introduced almost two decades ago as non-ionic uncharged analogue of phosphodiester oligomers, which are resistant to enzymatic degradation[104]. Similar to phosphorothioate derivatives, they feature substitution of one non-bridging oxygen atom of the internucleoside phosphodiester position by a methyl group, which results in creation of a new stereocenter at the phosphorus atom. However, there have been conflicting results with oligonucleotides containing this modified backbone. The later reports demonstrate formation of stable Pu*Pu.Py triple-stranded structures between oligopyrimidine phosphodiester RNA – r(T,C) and DNA – d(T,C) strands and stereorandom oligopurine d(A,G)-containing methylphosphonates[105,106], while such triplexes were not formed by the isosequential phosphodiester d(A,G) oligopurines[106]. In contrast it has been

reported that no triplexes were produced with d(A,T) mixtures when any of the strands consisted of methylphosphonates[107].

PNAs[108] are oligonucleotide analogues with a homomorphous, achiral, uncharged backbone and based on N-(2-amino-ethyl)glycine instead of deoxyribose phosphate as the repeating unit (Figure 14e). Homopyrimidine PNA was shown to bind to single- or double-stranded DNA forming a very stable DNA 2:1 complex with the purine target sequence[109]. Strand displacement happens when the complementary pyrimidine sequence is in the duplex target. This leads to formation of a P-loop structure, which inhibits transcription under physiological conditions. Oligopurine PNA is also capable of strand displacement forming a very stable 1:1 complex its oligopyrimidine DNA target sequence[110].

Recently, uniformly modified oligo-2'-deoxyribonucleotides containing internucleotide N3'→P5' phosphoramidate linkages have been synthesized. These modifications give a backbone that is ionised (negatively charged) at neutral pH similar to phosphodiester. *In vitro* and cell culture experiments show these modified phosphoramidates to be capable of forming Hoogsteen hydrogen bonds and with the very promising property of nuclease stability [111,112]. Compared with their phosphodiester counterparts, the oligo-2'-deoxynucleotide N3'→P5' phosphoramidates form more stable triplexes with complementary DNA strands. This has been observed in various reports[111-113]. However, highly stabilized triplex structures formed only with (T,C) and (T,G)-motifs bound in a parallel orientation with oligopurine sequence; the (G,A) or (G,T)-containing (PN) oligonucleotides seem to be unable to form stable triple helices in antiparallel orientation[114-116]. The C3'-*endo* nucleoside

sugar puckering, which is preferred by oligonucleotide N3'→P5' phosphoramidates and by native RNA, disfavours formation of required reversed Hoogsteen-type base pairs between targeted DNA oligopurine strand and the TFO.

Modifications to the sugar-position of the TFO are also able to increase resistance to nuclease enzymes and also improve the biological stability of the third strand. Several studies have shown that the chemical nature of the sugar has a dramatic influence on triplex-helix formation with the substitution of 2'-deoxyribose for ribose in the TFO being significant. In the pyrimidine motif, a more stable triplex is formed when the TFO is RNA rather than DNA[117-119]. This was observed for the (C,U) or (G,U)-motif with a parallel orientation of the third strand with respect to the purine target sequence[119]. Structure determination by ^{1}H NMR analysis was performed on short intramolecular hybrid triple structures with a RNA TFO in the (U,C) motif[120]. For parallel triplexes, only the pyrimidine TFO can be RNA, whereas for antiparallel structures RNA is not well tolerated unless all three strands of the triplex, the TFO and the duplex target, are RNA[102-104]. These observations have been explained by the suggestion that the binding affinities of RNA or DNA third strands to double helical nucleic acids are length, sequence composition, pH and salt-dependent[121]. A further stabilization of triplexes involves methylation of the 2'-OH groups in the third strand. The 2'-*O*-alkyl analogues have shown a higher stability than that of oligoribonucleotides[122]. Using a sulphur atom to replace the oxygen atom at the 4'-position of the sugar ring leads to a moderate stability increase when 4'-thio modifications are placed in contiguous stretches[123]. Substitution of the ring oxygen of 2'-

deoxycytidine with a carbon atom induces an increase of the pK_a value, which leads to a more pronounced increase in stability, whereas the triplex stability decreases when the substitution involves thymidine[124].

1.6.3 Covalent Attachment to TFOs

When added to triple-helical complexes, many ligands such as intercalators, minor groove binding agents or polycationic molecules have been shown to enhance triplex stabilities. A further stabilization increase can be obtained by covalently linking these molecules to the TFOs. However, this increase depends on many parameters, such as the size and nature of the linker between the two entities as well as the positions on the oligonucleotide and the ligand involved in the coupling. To provide TFOs with additional properties it is also possible to endow them with ligands able to induce irreversible modifications of the target sequence such as cleavage or covalent linking at specific sites. In this case, the best efficiency is achieved when both strands of the target DNA are modified. A few examples of these triplex-forming oligonucleotide-ligand conjugates are described below.

1.6.3.1 Covalent Linking to Intercalators, Groove Binders and Other Stabilizing Ligands

When attached to the 5'-end of a third strand oligonucleotide, 9-aminoacridine (Figure 15), and daunorubicin (Figure 16) derivatives have been shown to strongly stabilize the triplex formed with the DNA target by intercalation at the triplex-duplex junction[125,126]. New families of intercalators with a higher affinity for the triplex-helical rather than the double-stranded

complex are being developed. Among them, benzo[e]pyridoindole and benzo[f]pyridoquinoxaline derivatives have been covalently linked to pyrimidine third strands via flexible linkers of varying sizes at either the strongest stability increases were observed with a benzo[f]pyridoquinoxaline derivative conjugated to the 5'-end, and with a benzo[f]pyridoquinoxaline or a benzo[e]pyridoindole derivative benzo[g]pyridoindole linked to internucleotide positions of the oligonucleotides[127,128], respectively. The relevant structures are shown in Figure 15.

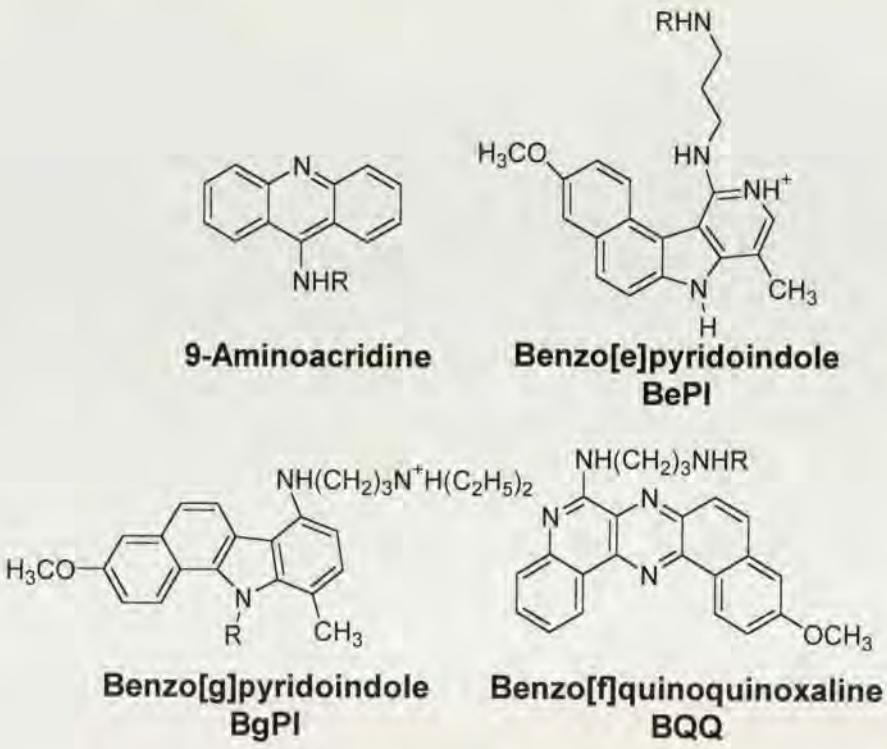

Figure 15. DNA triplex binding ligands (I), R is the point of the attachment of the ligand to the TFO.

Hoechst 33258 (Figure 16), a minor groove binder, has also been covalently linked to the 5'-end of a pyrimidine third strand[129]. Complex stabilization by

simultaneous major and minor groove binding has been observed. In the same way, the covalent coupling to a pyrimidine third strand of a minor groove binding ligand composed of polyamides containing *N*-methylimidazole and *N*-methylpyrrole amino acids, combined side-by-side, leads to an increased stability of the triple-helical complex[130]. When linked to the 5'-ends[131] or at the N-4 position of an internal cytosine[132] of TFOs oligonucleotides, spermine (Figure 16) stabilizes the triplex, as do cationic peptides linked to the 5' -ends of pyrimidine third strands[133].

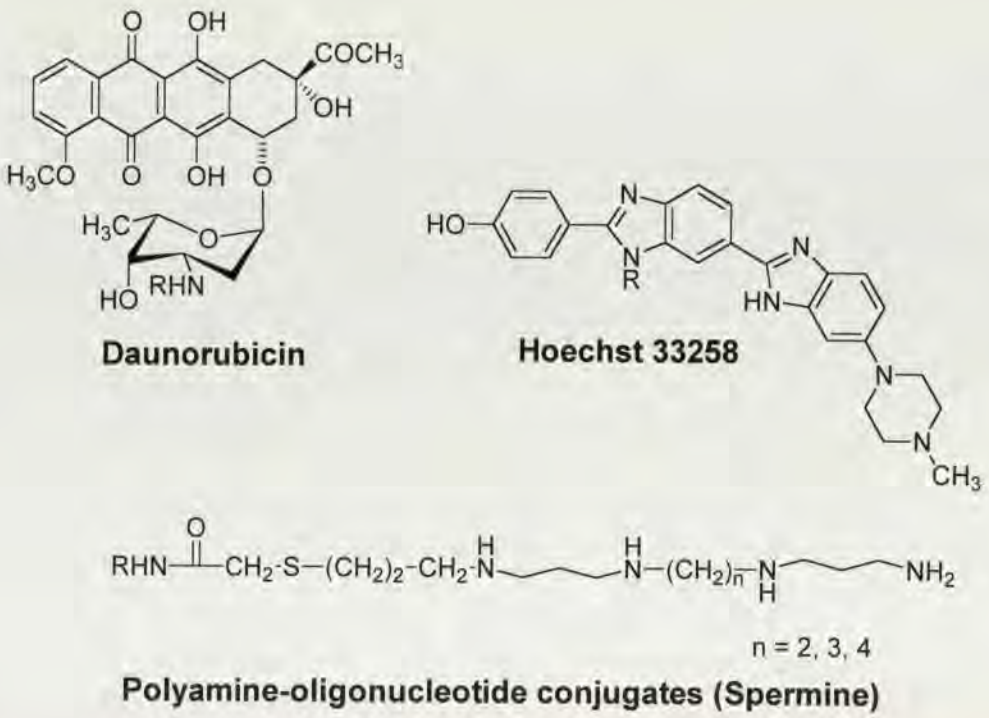

Figure 16. DNA triplex binding ligands (II), R is the point of attachment to the TFO.

1.6.3.2 Covalent Linking of Alkylating and Cleaving Reagents to the Third Strand

Even though certain TFOs modified at the level of the oligonucleotide chain and covalently linked to intercalators are able to form stable triplexes under physiological conditions, they can be displaced by replication or transcription machinery. One way to improve the potential of the triple helix forming oligonucleotides in regulating gene expression is to attach to them reagents able to induce irreversible modifications of the target sequence such as cleaving or crosslinking[118]. A variety of reactive groups have been used in order to cleave the DNA target or to link the triple helix forming oligonucleotides to their specific binding sites. These reagents can be divided into three groups. The first group concerns metal chelates Fe-EDTA, Fe-porphyrin, Cu-orthophenanthroline and more recently Fe-bleomycin[134], which induce cleavage of the target via oxidative degradation of the deoxyribose ring. The second group includes compounds such as psoralen and azido-containing compounds, which are able to induce a covalent bond between the TFO and the target under irradiation. These reagents do not require cofactors and are not reactive until activated by light. Psoralen-oligonucleotide conjugates that are resistant to nucleases have been used to demonstrate that the DNA target sequence is accessible in the cell nuclei[112]. The last group involves alkylating compounds, which are able to react spontaneously with the target via electrophilic alkylation of the bases. Among them the most attractive for *in vivo* applications are those that are chemically stable when tethered to a single strand oligonucleotide but very reactive after hybridisation of the oligonucleotide with its target. More recently the *N*-5-

methylcyclopropapyrroloindole residue, a structural analogue of cyclopropapyrroloindole the reactive subunit of the potent antibiotic CC-1065, which alkylates adenines at their N-3 position, has been linked at both the 5'- and 3'- positions of a purine third strand. This conjugate has the proven capability of alkylating, efficiently and quickly, in physiological buffer, both strands of the target duplex region immediately adjacent to its binding site on the double-stranded target[135]. By analogy with the RNase H-mediated activity of antisense oligonucleotides, an alternative way for biological applications would be the recruitment of a cellular enzyme, which would be directed to perform a sequence-specific cleavage of the target DNA. When covalently linked to the 3'-end of a pyrimidine third strand, camptothecin, an inhibitor of topoisomerase I, has been proven to induce *in vitro* sequence-specific cleavage of one strand of the double-stranded DNA target by topoisomerase I[136].

1.7 Pyridine-Stretched Bases (PSBs)

As discussed above, a lot of studies have been directed at improving triplex stability in different positions of TFOs[137,138]. Work described in this thesis involves a different strategy: improving the triplex stability with new pyridine-stretched, tricyclic analogues of the DNA bases. Recent studies from a current Aston-Keele collaboration have aimed to develop new TFOs containing novel pyridine-stretched bases (PSBs) for ultimate use in the control of gene expression at the level of transcription[139]. PSBs are linear, tricyclic analogues of the familiar DNA purine bases where a central pyridine ring connects the 6-membered pyrimidine ring to the 5-membered imidazole

ring, which is in turn attached to the anomeric C1' carbon of 2-deoxyrobose[139] (Figure 17).

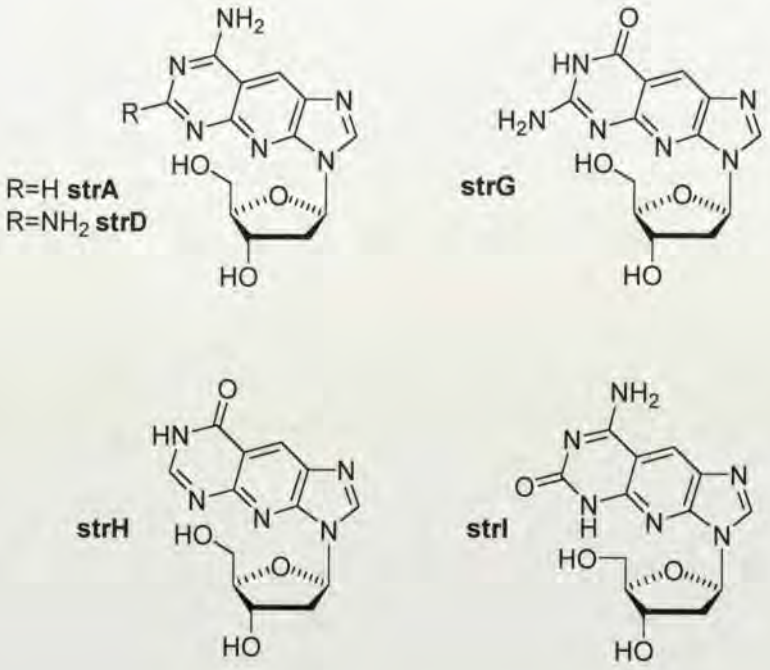

Figure 17. The PSBs analogues of the nucleic acid purine bases. adenine (R=H; strA), diaminopurine (R=NH_2; strD), hypoxanthine (strH), guanine (strG) and isoguanine (strI).

PSBs with their tricyclic structure are expected to show, theoretically, a higher base stacking contribution to triplex stability compared with the natural purine and pyrimidine structures. Base stacking interactions provide significant stabilisation of single-, double- and triple-stranded DNA. Increased base-stacking contributions have been shown to improve hybrid stability of 5-propynyl[10] and phenoxazine[140] derivatives of cytosine. The basis of the stability increase predicted for PSBs is increased π-σ attraction between adjacent faces of the tricyclic ring system. Figure 18 provides a structural rationale for this additional overlap. The two adjacent PSB rings modelled onto a canonical A-form helix possess substantial overlap between

the second ring of one tricycle and the third ring of the adjacent tricycle (Figure 18c). Such extensive overlap is not possible in analogues of less than three rings. The corresponding pyrimidine-pyrimidine overlaps shown in Figure 18a and purine-purine overlap shown in Figure 18b are substantially less[140].

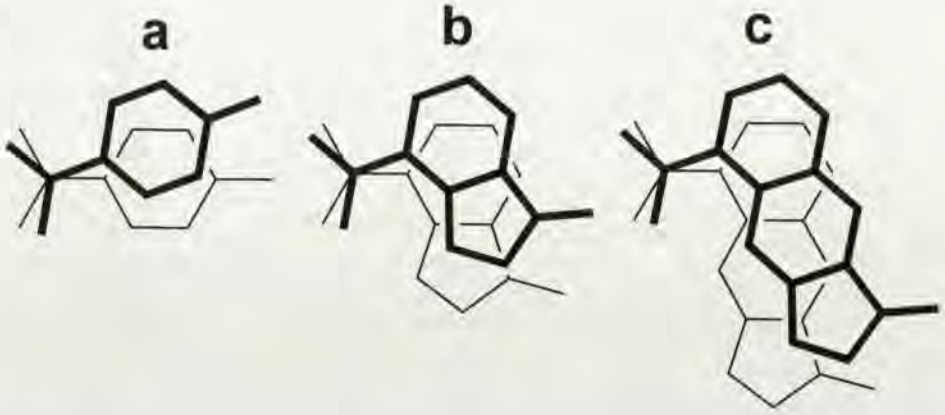

Figure 18. Over lap of adjacent bases: (a) pyrimidine-pyrimidine; (b) purine-purine; (c) PSB-PSB in a canonical A-form duplex. Viewing perspective is down the axis of the helix in a 5' to 3' direction, with the bold image being above.

In addition to the favourble base stacking that the PSBs potentially offer, other improvements to triplex stability could include the following. The choice of isomorphous base combinations such as strI and strH might lessen backbone distortion in the TFO. No extra protonation of the PSBs is required meaning stability over a wider pH range. Compared with the DNA bases, PSBs are longer therefore the TFO backbone is likely to be positioned further away from the target duplex, which may lessen electrostatic repulsion between backbones. Other features that may have a bearing on the triplex stability of PSOs include sugar conformation and the basicity of the central pyridine nitrogen atom. Both of which are difficult to predict beforehand and could aid or hinder triplex stability.

1.8 Oligonucleotide Synthesis

To form new PSOs containing strD, automated solid phase synthesis needs to be performed. This should be possible using a standard DNA synthesizer and phosphoramidite chemistry. The process is shown in Figure 19 and typically involves the following steps. The protected nucleotide is covalently bound to a solid support, and one nucleotide at a time is added to the chain by use of tetrazole or analogous coupling reagent.

The first step in oligonucleotide synthesis involves attaching a protected deoxynucleoside to a solid support by an ester linkage to the 3'-OH group of the deoxynucleoside. Both the 5'-OH group on the sugar and any free $-NH_2$ groups on the heterocyclic bases must be protected. The deoxyribose 5'-OH is protected as its *p*-dimethoxytrityl (DMT) ether.

Next is the removal of the DMT protecting group by treatment with dichloroacetic acid in CH_2Cl_2. The reaction occurs by an S_N1 mechanism and proceeds rapidly because of the stability of the tertiary, benzylic dimethoxytrityl cation produced.

The third step involves coupling of the polymer-bound deoxynucleoside with a protected deoxynucleoside containing a phosphoramidite group at its 3' position. Any unreacted 5'-OH sites are acylated to prevent further reaction and build up of failed sequences.

The phosphite product is oxidized to a phosphate by treatment with aqueous iodine. The cycle of detritylation, coupling, and oxidation is then repeated until an oligonucleotide chain of the desired sequence has been built.

The final step is removal of all protecting groups and cleavage of the ester bond holding the DNA to the solid phase support. All of these reactions can

be done at the same time by treatment with aqueous NH_3, if base-labile protecting groups are employed. Purification by HPLC then yields the synthetic oligonucleotide product.

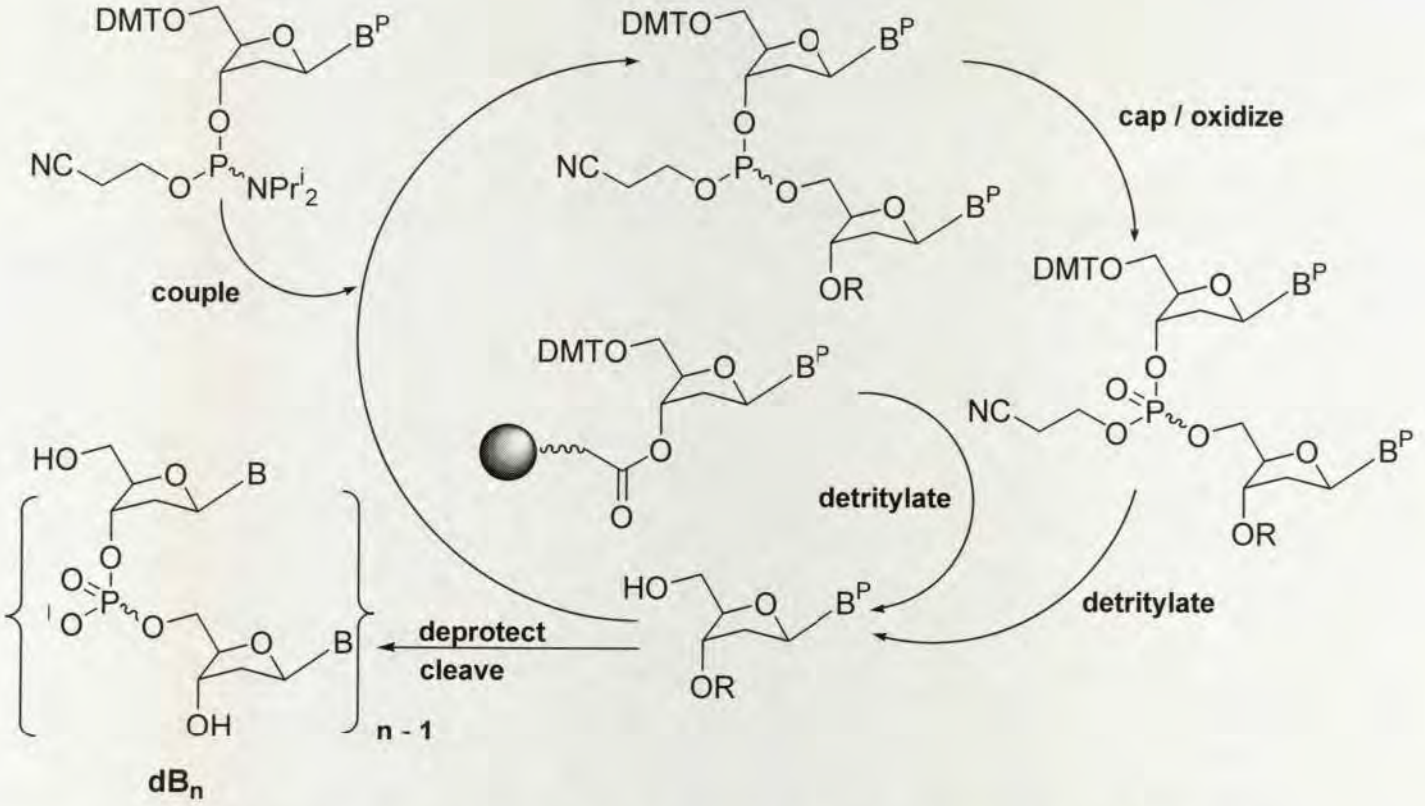

Figure 19. Synthesis cycle for the preparation of oligonucleotides by the phosphoramidite method.

Discussion and Results

2.1 Choice of Chlorosugar 4

The well known 1'-chloro-2'-deoxy-3',5'-di-*O*-toluoyl-α-D-*erythro*-pentofuranose **4** has proven to be an good reagent for the synthesis of 2'-deoxyribonuclesides, readily coupling with the anion of the appropriate base[141,142]. However, refrigeration is crucial to avoid decomposition of **4** on prolonged storage as the HCl produced on hydrolysis can adversely affect glycosylation. Recent work on the preparation of this compound, as the crystalline α-anomer in three steps from 2'-deoxyribose **1**, has resulted in improved yields (Scheme 1). The formation of only the α-anomer **4** is the key factor in this process. The reason that only one anomer is formed, is due to the anomeric effect[143]. This effect is caused by the donation of electrons from a non-bonding orbital on the ring oxygen atom in to the σ* orbital of the adjacent carbon-chloride bond. The orientation of the oxygen non-bonding orbital means that this effect can only be seen in the α-anomer. The strength of the anomeric effect is dependant upon the σ* orbital of the bond between the anomeric carbon and its substituent. The greater the polarity of this bond, the larger the σ* orbital and thus the larger the anomeric effect. Where the substituent is a halogen, in this case chlorine, the effect is so strong that only one anomer is seen.

2.2 Synthesis of Chlorosugar 4

According to the synthetic route described in Scheme 1, 2'-deoxyribose **1** was reacted with acetyl chloride to give 2′-deoxy-1′-*O*-methyl-α/β-D-

erythro-pentofuranose **2** in a 99% yield. The hydroxyl groups in **2** were protected with toluoyl groups to give 2'-deoxy-1'-(3',5'-di-*O*-toluoyl)-*O*-methyl-α/β-D-*erythro*-pentofuranose **3** in a high yield (96%). Compound **3** underwent chlorination at C1' with acetic acid saturated with HCl to give chlorosugar **4** in 62% overall yield from **1**.

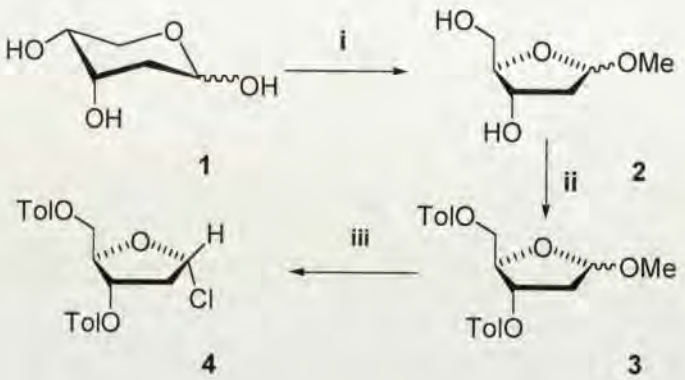

Scheme 1. Reagents and conditions: **i**, MeOH/CH_3COCl/rt; **ii**, p-toluoyl chloride/pyridine/0 °C to RT; **iii**, HCl/AcOH/15 °C.

2.3 Glycosylation of 4 Using Cesium 4(5)-Nitroimidazole

For the glycosylation reaction (Scheme 2), to give only the one desired anomer **6**, stereo-specific control is required. When the glycosylation was performed, four different isomers were found and identified by ^{1}H-NMR and NOSEY[139] (Figure 20) (**6-9**). ^{1}H-NMR spectra showed each H-1' proton 5-nitro-1'-β (triplet, δ = 6.74 ppm), 5-nitro-1'-α (doublet, δ = 6.80 ppm) downfield relative to those of the 4-nitro-1'-β (triplet, δ = 6.15 ppm) and 4-nitro-1'-α (doublet, δ = 6.25 ppm) signals. Formation of the β-anomers **6** and **7** probably proceeds by an S_N2 Walden inversion process at C1' (Figure 21a). This is presumably the preferred mechanism in the absence of a neighbouring 2'-acyl group, which can normally participate in the glycosylation reaction to

give exclusively β products. Formation of the α-anomers **8** and **9** can be explained by a similar process, if the chlorosugar **4** first anomerises to the β configuration at C1' before reaction with the base (Figure 21b).

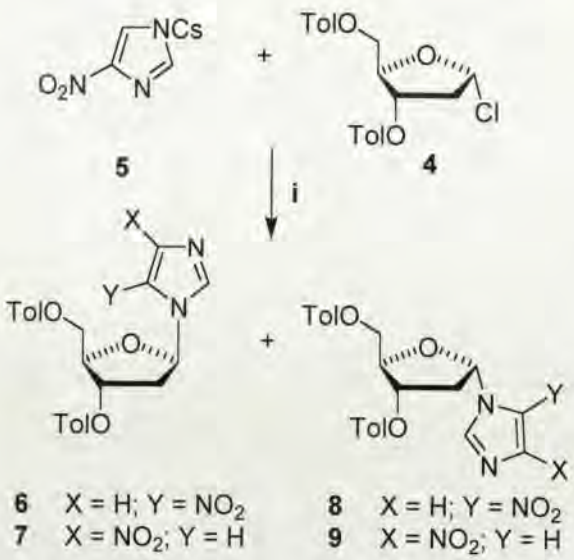

Scheme 2. Possible isomeric products from glycosylation of **5** using **4**. Reagents and conditions: **i**, THF/62 °C.

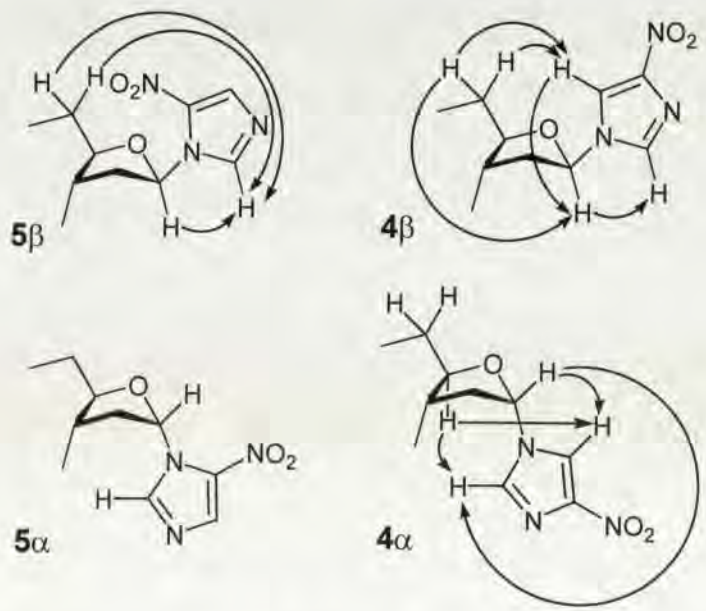

Figure 20. A summary of NOEs derived from NOESY spectra of the isomers.

The synthetic route that is shown in Scheme 2, required optimisation to maximise the yield of **6**. To improve the yield of 1-(2-deoxy-3,5-di-*O*-*p*-toluoyl-β-D-ribofuranosyl)-5-nitroimidazole **6**, various solvents and conditions were explored. In previous glycosylations to prepare the ribonucleoside, Ramsden and co-workers[144] employed the silver salt and lithium salt of ambident nucleophile 4(5)-nitroimidazole in different solvents. However, the yield of **6** using these conditions was suboptimal. Bergstrom and co-workers[145] performed glycosylation of **4** under standard conditions where the sodium salt of 4(5)-nitroimidazole reacted with chlorosugar **4**, β- and α-anomers were isolated in a 1:2 ratio. All results indicated that the choice of solvent, nucleophile and concentration strongly influenced the yield distribution of the four different isomers (**6-9**).

It was suggested that the anomerisation of the chlorosugar **4** occurs readily with solvents of higher dielectric constant and is further enhanced by the presence of lithium, silver and to a lesser extent sodium ions[146,147]. For the purpose of minimizing isomerzation, the cesium salt of 4(5)-nitroimidazole was employed in this reaction. Cesium is less likely to co-ordinate to the 1'-chloro substituent and is unlikely to enhance anomerisation of the chlorosugar **4**. Solvents tried were toluene, THF and acetonitrile at room temperature and at reflux. The outcomes of the experiments are shown in Table 1. Toluene gave almost no product at room temperature, and at 62 °C gave primarily the unwanted β-anomers **8** and **9**. Acetonitrile at room temperature was found to give the desired product, but the yield of **6** was not practicable enough to supply the necessary gram quantities of starting

material. THF gave the highest isolated yield of desired product (>70%) when freshly prepared starting materials were used and the reaction carried out under argon at 62 °C for 2 hours.

Table 1. Reaction conditions and relative proportions of (**6-9**) for the synthesis of compound **6**.

Solvent	**Temp. (°C)**	**Time (h)**	**% of isomers**			
			5β	5α	4β	4α
THF	50	2	43	16	28	13
THF	62	2	54	15	28	3
THF	80	2	57	12	30	1
THF	62	2	71	6	20	3
CH_3CN	rt	0.5	43	0	57	0
Toluene	62	3	23	18	44	15
Toluene	rt	2	21	8	54	17

Relative proportion based on integration of each CH-1' peak from proton NMR analysis.

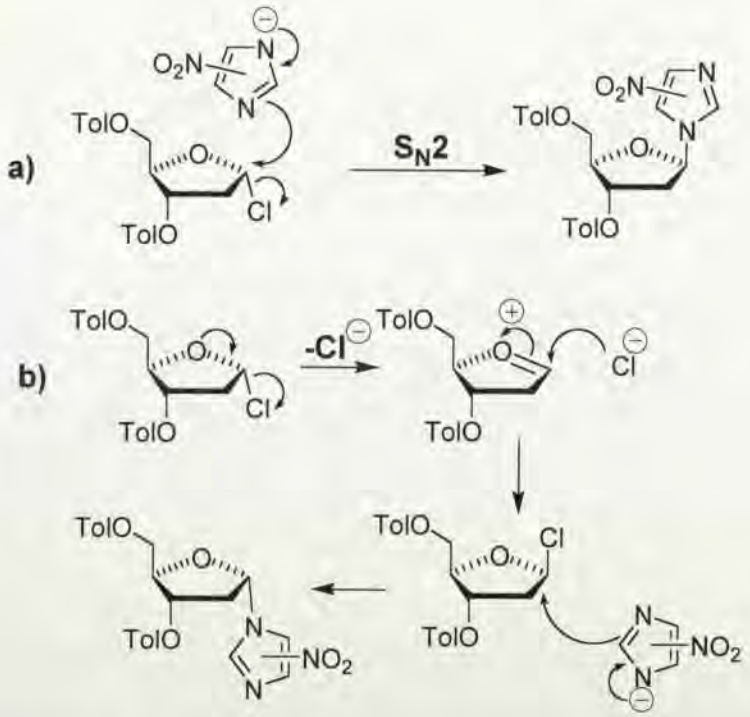

Figure 21. Mechanism of glycosylation reaction; **a**) β-anomer formation; **b**) α-anomer formation.

1-(2-Deoxy-3,5-di-*O*-*p*-toluoyl-β-D-ribofuranosyl)-5-nitroimidazole **6** was characterized using ^{1}H-NMR and NOESY spectra[139]. Two methyl peaks were seen, corresponding to the toluoyl groups. Ten aromatic protons accompanied these. Eight had been previously seen for the toluoyl groups in **4**; the two new peaks correspond to the nitroimidazole functionality. The presence of a triplet as opposed to a double at 6.74 ppm corresponds to the β-anomer product.

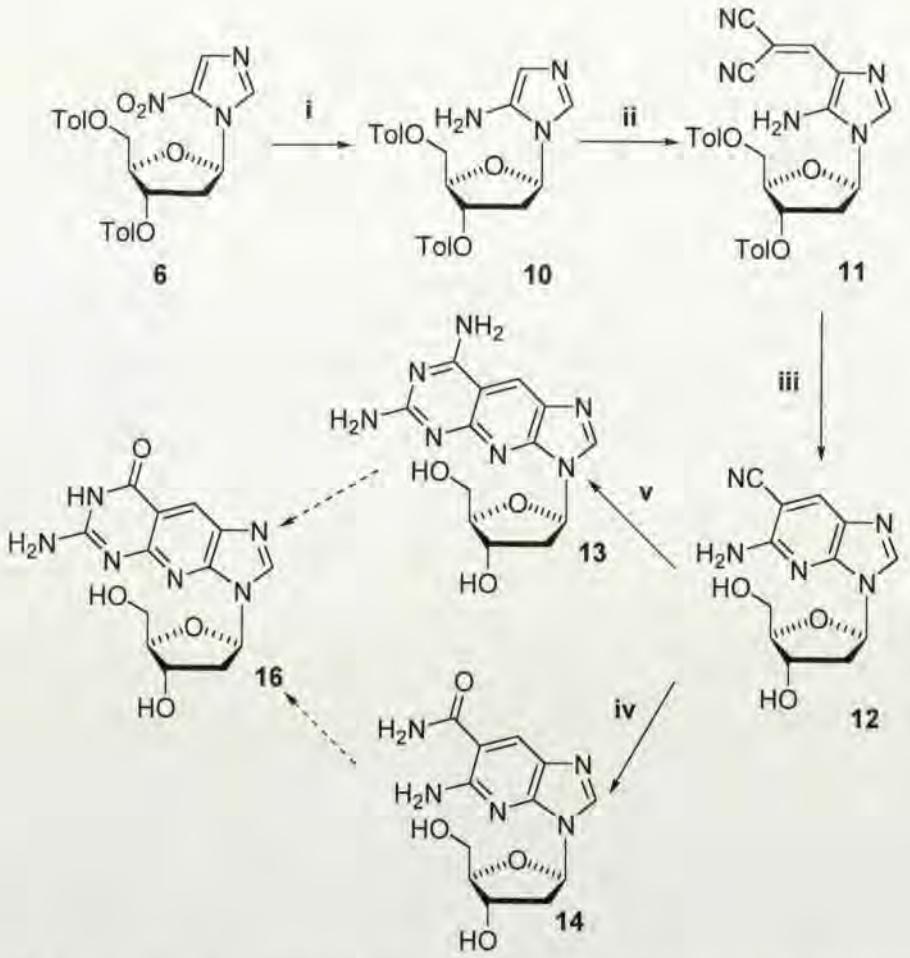

Scheme 3. Proposed route to strD. Reagents and conditions: **i**, H_2/Pd on C/rt; **ii**, EtOCH=C(CN_2)/THF/rt; **iii**, MeOH/NaOH/60 °C; **iv**, H_2O_2/NH_4OH, 20 °C/40 min; **v**, guanidine hydrocholoride/MeONa/MeOH/140 °C.

2.4 Hydrogenation of Nitroimidazole Nucleoside 6 and Direct *C*-Alkylation to Nucleoside 11

Ramsden *et al*[148] reported that THF and 1,4-dioxane were good solvents for the catalytic hydrogenation of nitroimidazoles to their corresponding amines. Reactions in ethanol showed a number of significant by-products. In this work we found compound **6** was more soluble in THF; a solvent unaffected by the hydrogenation. The results of reduction of **6** carried out in THF were promising. The requisite volume of hydrogen was consumed each time and reaction progress was checked by TLC. The amine product showed only a

very faint yellowing. However, the amine rapidly discoloured to dark red during filtering and checking with TLC showed two spots. This indicated that the amine decomposed quickly in the air, so subsequent reductions were followed by direct alkylation to avoid contact of **10** with any air (Scheme 3). The addition-elimination reagent, ethoxy methylene malononitrile (EMMN), was then added in 40% excess to **10** and the solution stirred under argon for twelve hours to form the addition-elimination product 5-amino-4-(2,2-dicyanoviny)-1-(2-deoxy-3,5-di-*O*-*p*-toluoyl-β-D-ribofuranosyl)-imidazole **11** (Scheme 3).

After 12 hours the solution was concentrated and washed with chilled ethyl acetate. The yellow powder **11** was obtained in 43% yield from **6** over two steps. This yield is the best to date and, although not optimal, is practicable. Chromatography has been tried, to remove the impurities from the crude material, but it was believed that the chromatography decomposed the product slightly. To overcome this, a solvent was sought that allowed the addition-elimination product to precipitate. After trying a number of solvents, it was found that EtOAc had the desired property. Compared to using chromatography, the precipitation method gave better yield. The outcomes of the various attempts at the addition-elimination reaction are summarized in Table 2.

Table 2. Attempts at the addition-elimination reaction in different temperature and different precipitation solvent.

Temp. (°C)	Time (h)	Precipitation solvent	Yield (%)
-50	12	EtOAc	5
0	12	EtOAc	23
rt	12	EtOAc	43
rt	12	MeOH	30
rt	12	$CHCl_3$	27

The ^{1}H-NMR spectrum of compound **11** showed only one initially noticeable change from the starting material, the appearance of a broadened, D_2O exchangeable proton at 7.7 ppm. This peak was attributed to the amine group at the 5-imidazole position. There were still ten aromatic protons, eight of which were from the toluoyl groups. One was from the H-2 of the imidazole and the other corresponded to the vinyl proton of dicyanovinyl unit. Ramsden *et al*[144] have shown that 4-unsubstituted-5-aminoimidazoles are *N,C*-ambident nucleophiles and that soft electrophiles react on the imidazole ring to give 4-substituted products. In contrast, hard electrophiles add to the exocyclic nitrogen atom with the relative sizes of HOMO coefficients and the charge distribution in 5-aminoimidazoles[149] (Figure 22). Since the reagent EMMN is classified as soft, the formation of the C-C bond at the 4-position of the imidazole ring of **10** to give compound **11** is preferred over *N*-alkylation (Figure 23).

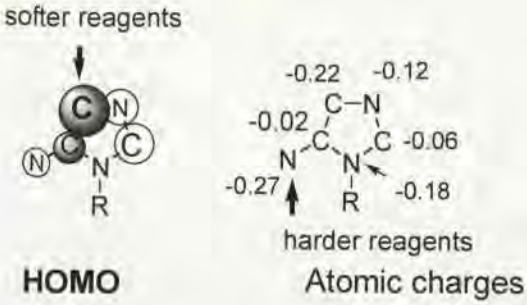

Figure 22. 4-Unsubstituted-5-aminoimidazoles are *N,C*-ambident nucleophiles.

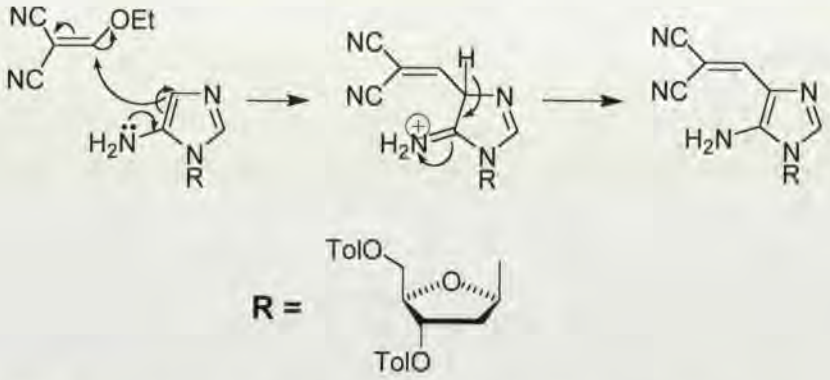

Figure 23. Proposed mechanism of the *C*-alkylation of **10** to form **11**.

2.5 Cyclisation of Dicyanonucleoside 11 to Nucleoside 12

The next step, conversion of **11** to **12**, presented the choice between cyclisation to form the pyridine ring (Scheme 3) with the sugar still protected or with concomitant deprotection. As mentioned in Ramsden's literature, and supported by work at Aston, similar deprotection steps utilizing an amine base or with $NaHCO_3$ at room temperature are slow and only appeared to remove one of the two toluoyl protecting groups. To combat this problem it was decided to use a stronger base, at elevated temperatures, if required. Ramsden *et al*[148] had used a methanol-water-sodium hydroxide mixture for the cyclisation. These conditions are typical for ester hydrolysis, cyclisation and deprotection. From this idea it was decided to use a 5% (aq) sodium

hydroxide solution and combine the two steps, hydrolysis (deprotection) and cyclisation. The sodium hydroxide was used in large excess, due to the slow rate of previous attempts at cyclisation, and because of the fact that the hydroxylation is used up in stoichiometric amount as the deprotection reaction progresses.

TLC was used to monitor the reaction and almost immediately the spot corresponding to the starting material **11** disappeared to give a new fluorescent spot at a slightly lower R_f. This spot then slowly faded as two lower fluorescent spots were seen. After approximately 15 min only a dark spot at the top of the plate, believed to be the removed toluoyl moiety, and a fluorescent spot low on the plate, remained. With another 15 min for the reaction, slight fluorescent spot was found on the plate with lower R_f. It seems feasible that the cyanide group of **12** could react with the excess base, therefore neutralization with citric acid was very important to maintain the product yield (84%).

The ^{1}H-NMR spectrum of this compound (**12**) was straightforward to interpret because distinct proton peaks, without any overlapping, were seen. There are two aromatic protons for the pyridine and imidazole protons and a slightly broadened singlet at 6.8 ppm corresponding to the amine protons. Both the hydroxyl protons at positions 3' and 5' are seen at 4.4 and 5.0 ppm respectively. These were assigned by using their multiplicity, a doublet for the secondary hydroxyl and a triplet for the primary hydroxyl group. Then protons at positions 3' and 4' are seen at 5.3 and 3.8 ppm respectively, and a multiplet is observed at 3.5 ppm for the two 5' protons. Finally the two H-2' protons are seen as two separate multiplets at 2.6 and 2.2 ppm.

2.6 Cyclisation of Nitrile Nucleoside 12 to strD 13

Reaction of **12** to form compound **13** using guanine hydrochloride has been attempted using different conditions. A number of relevant literature methods involving analogues were considered[150-154]. For the cyclisation, high temperature should be employed. Temperatures ranged from 60-145 °C and the reaction attempted repeatedly at increasing 20 °C intervals. Only at 145 °C did the reaction proceed satisfactorily (2 days) and with guanine as its free base, generated from its hydrochloride salt at the start of the reaction. TLC analysis using EtOAc-MeOH (10:1) showed that the starting material disappeared. The isolated yield of **13** was 45% and its structure is supported by its spectroscopic properties. The solvent for the reaction has also been considered. Of the solvents tested, the starting material only dissolved in MeOH, although relevant literature reports use high boiling point solvents for other analogues. To avoid evaporation of MeOH at 145 °C, a metal bomb was used to carry out this reaction. An excess of guanidine was needed and, as the free base, proved air-sensitive for this reaction. At the same time, the metal bomb, allowed exclusion of air. The likely mechanism for the cyclisation reaction is shown in Figure 24.

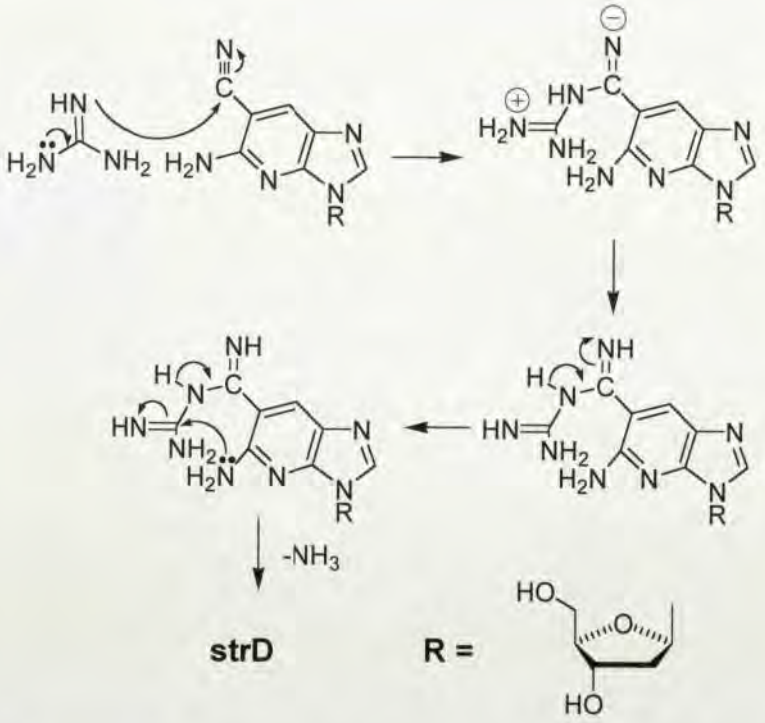

Figure 24. Proposed mechanism of the cyclisation reaction of **12** to form strD **13**.

2.7 Evaluation of Different Synthetic Routes to strG

For the synthesis of strG three alternatives are suggested as viable synthetic routes (Scheme 4). Alkaline hydrolysis of strG[151-153] would be the most direct and potentially efficient way. But competition between the two amino-substituted centres could give a mixture of strG and its regioisomer, strI. If hydrolysis proves low yielding, troublesome or unviable due to preferred hydrolysis of the alternative 2-NH_2 position, then the two remaining routes, although longer, seem worth exploring. According to the literature,[155-157] isocytosines can be prepared from 1,3-dimethyluracils by reacting with guanidine (Figure 25). The success of this process is dependant upon the substituents at C5 and C6. The reaction proceeds with guanidine in boiling ethanol when an electron substituent (F or Br) is attached at C5. Based on this

idea, conversion of **14** to **16**, via **15a** and **15b** should lead to strG. The last synthetic route from **14** direct to **16** has been well described by Leonard[158,159] for similar structures.

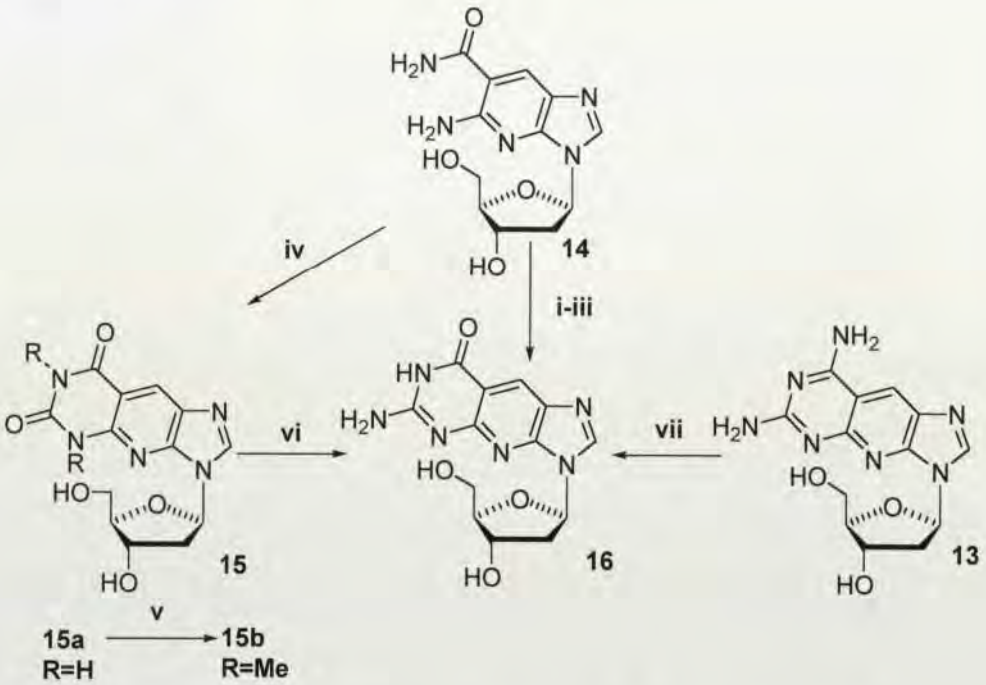

Scheme 4. Three proposed synthetic routes to strG. Likely reaction conditions: **i,** MeOH/NaOH/CS_2; **ii,** H_2O_2; **iii,** NH_3; **iv,** $OC(OEt)_2$; **v,** $(MeO)_2CHNMe_2$; **vi,** $HN{=}C(NH_2)_2$; **vii,** HCl/$NaNO_2$.

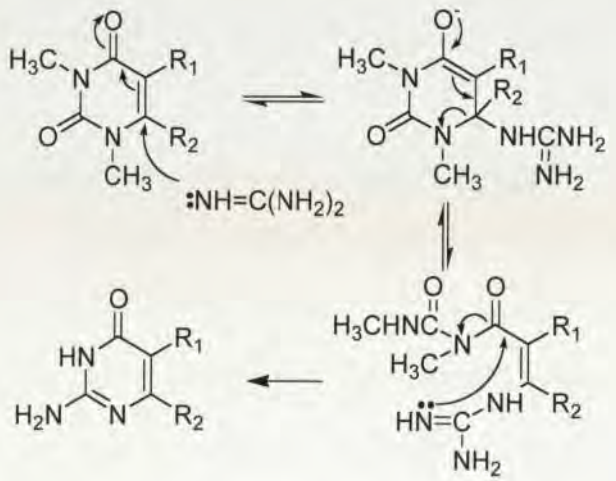

Figure 25. Mechanism for isocytosine (R_1 = R_2 = H) synthesis from 1,3-dimethyluracil.

2.8 Proposal for StrD Phosphoramidite Synthesis

Although not performed in this thesis work due to limitations of time, the following scheme (Scheme 5) outlines the necessary derivatisation of strD to give the required phosphoramidate binding block for use in solid phase synthesis of PSOs containing strD.

In the Scheme 5, use of the *tert*-butylphenoxyacetyl[160] group to protect the exocyclic amino groups of strD, dimethoxytriylation of the 5'-OH group and phosphitylation of 3'-OH using 2-cyanoethyl-*N*,*N*-diisopropyl chlorophosphoramidite are necessary to give the required strD phosphoramidite.

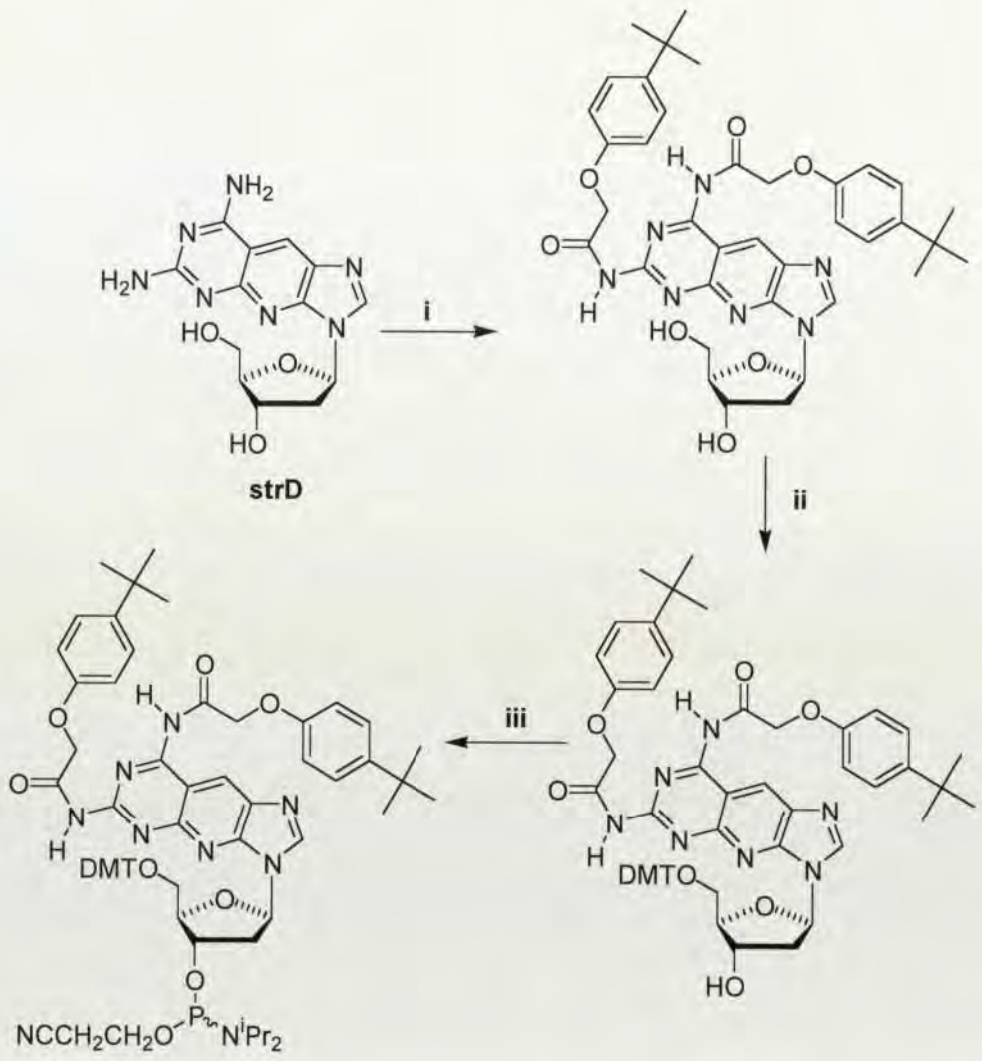

Scheme 5. Reagents: **i**, 4-*tert*-butylphenoxyacetyl; **ii**, DMTCl, C_5H_5N; **iii**, $NCCH_2CH_2OP(Cl)NPr^i_2$, Pr^i_2NET THF.

2.9 Conclusion

The initial glycosylation of the starting material (Scheme 1) was the focus of a lot of chemical effort but is now straight forward, with conditions[1] clearly defined that give a good yield of the desired nitroimidazole isomer **6**. The hydrogenation of **6** to give the amino nucleoside **10** was successfully achieved, but direct alkylation is necessary to allow for the instability of **10**. The alkylation reaction is still a low yielding despite repeated attempts to

optimize. It was believed that the aminoimidazole nucleoside behaves as an N, C ambident nucleophile towards EMMN and although C-alkylation was the aim, possible N-alkylation or formation of other by-products might account for the low yield of **11**.

The cyclisation of **11** to **12,** with concomitant deprotection of the sugar was straightforward. The cyclisation of **12** to strD **13** using guanidine free base was achieved after some experimentation, in reasonable yield. All compounds have been fully characterised spectroscopically, and their analytical data supports all of the proposed structures.

Subsequent hydrolysis of strD to strG and alterative routes to strG have been proposed.

Experimental

General: NMR spectra were recorded on a Bruker AC-250 spectrometer at ^{1}H (250.1 MHz) and ^{13}C (62.9 MHz) with positive chemical shifts downfield of TMS (^{1}H, ^{13}C). Mass spectra were recorded using VG Quatro II or VG AutoSpec instruments. Flash column chromatography[161] was performed using Sorbsil C60 silica and TLC was performed using plastic-backed Kiesegel 60 silica plates containing a fluorescent indicator and visualized under UV (254 nm) and with acidic vanillin solution.

2′-Deoxy-1′-*O*-methyl-α/β-D-*erythro*-pentofuranose 2

To a solution of 2-D-deoxyribose **1** (25 g, 186.6 mmol) in MeOH (375 mL), a solution of acetyl chloride (0.84 mL, 12.3 mmol) in MeOH (42 mL) was slowly added at rt. After 10 min stirring, $AgCO_3$ (8.17 g, 29.6 mmol) was added and stirring continued for a further 5 min. The resultant mixture was filtered through Celite and concentrated under reduced pressure, then dried under high vacuum to yield the crude product **2** (27.35 g, 184.8 mmol), (99%) as colourless oil. TLC analysis (EtOAc/MeOH 4:1) R_f 0.40, ^{1}H-NMR ($CDCl_3$): δ 2.19 (2H, m, 2-C*H*$_2$), 3.37 (1.5H, s, 1-OC*H*$_3$), 3.39 (1.5H, s, 1-OC*H*$_3$), 3.66 (2H, m, 5-C*H*$_2$), 4.01 (1H, q, 4-C*H*), 4.09 (1H, m, 3-C*H*), 4.16 (1H, m, 1-C*H*), 4.37 (1H, s, 5-O*H*), 5.10 (1H, m, 3-O*H*).

2'-Deoxy-1'-(3',5'-di-*O*-toluoyl)-*O*-methyl-α/β-D-*erythro*-pentofuranose 3

The pentofuranose **2** (27.35 g, 184.8 mmol) was dissolved in dry pyridine (190 mL), and cooled to 0 °C under Ar. *p*-Toluoyl chloride (54 mL, 15.24 mmol) was added dropwise in 70 min to a stirring solution of **2** in pyridine. The cooling bath was removed after 40 min and stirring continued overnight at rt. The reaction mixture was evaporated under reduced pressure and concentrated under high vacuum. The residue was partitioned between ether and water and organic layer washed with 0.1 M HCl (aq.) followed by saturated $NaHCO_3$ (aq.). The ether layer was dried over anhydrous $MgSO_4$ and concentrated under high vacuum to yield the product **3** (67.97 g, 177.0 mmol, 96%) as a soft pale yellow crystalline solid. TLC (EtOAc-MeOH 4:1): R_f 0.74. ^{1}H-NMR ($CDCl_3$): δ 2.40 (8H, m, 2'-C*H*$_2$, 2 x *p*-tol-C*H*$_3$), 3.36 (1.5H, s, 1'-β-OC*H*$_3$), 3.43 (1.5H, s, 1'-α-OC*H*$_3$), 4.45 (2H, m, 5'-C*H*$_2$), 5.22 (1H, m, 4'-C*H*), 5.41 (1H, m, 1'-C*H*), 5.61(1H, m, 3'-C*H*), 7.23 (4H, m, 2 x *p*-tol-C*H*), 7.97 (4H, m, 2, 6- *p*-tol-C*H*).

1'-Chloro-2'-deoxy-3', 5'-di-*O*-toluoyl-α-D-*erythro*-pentofuranose 4

Acetic acid (500 mL) was saturated with HCl and the solution cooled to 10-15 °C. The pentofuranose **3** (67.97 g, 177.0 mmol) was added as a solution in acetic acid (45 mL) with mechanical stirring. After stirring for a further 20 min, the mixture turned green. The precipitate was filtered, washed with ether (2 × 20 mL) and dried under high vaccum overnight, yielding the product **4** (43.90 g, 113.0 mmol, 65%). TLC (EtOAc-MeOH 4:1): R_f 0.83. ^{1}H-NMR ($CDCl_3$): δ 2.42 (6H, s, 2 x *p*-tol-C*H*$_3$), 2.78 (1H, m, 2'-C*H*), 2.85 (1H, m, 2'-

C*H*), 4.62 (1H, m, 5'-CH_2), 4.67 (1H, m, 5'-C*H*), 4.78 (1H, m, 4'-C*H*), 5.57 (1H, m, 3'-C*H*), 6.37 (1H, d, 1'-C*H*), 7.25 (4H, q, 3,5-*p*-tol-C*H*), 7.96 (4H, q, 2,6-*p*-tol-C*H*).

4-Nitroimidazole Cesium Salt 5

4-Nitroimidazole (15 g, 0.133 mol) was stirred with 150 mL MeOH at room temperature. To this was added cesium hydroxide (aq.) (50% by wt., 23.2 mL, 0.133 mol) drop-wise. After a further 1 h stirring the reaction mixture was evaporated under reduced pressure. The residue was recrystallised from *iso*-propanol and dried under high vacuum to yield yellow crystals of 4(5)-nitroimidazole cesium salt (23.8 g, 73%). ^{1}H-NMR [$(CD_3)_2SO$]: δ 7.07 (1H, s, C*H*), 7.68 (1H, s, C*H*); ^{13}C-NMR [$(CD_3)_2SO$]: δ 132 (*C*H), 146 (*C*H); MS (APCI$^-$) *m/z* 122 (M^-).

1-(2'-Deoxy-3',5'-di-*O*-toluoyl-α/β-D-*erythro*-pentofuranosy)-5-nitroimidazole 6

The chlorosugar **4** (5 g, 12.89 mmol) was dissolved in dry THF (500 mL) and the cesium salt **6** (6.37 g, 25.78 mmol) as added dropwise over 2.5 h with reflux and the resultant mixture was stirred at 62 °C. After stirring overnight at rt, the reaction mixture was filtered under reduced pressure and washed with THF (2 × 20 mL). The washings were dried under high vaccum to yield a crude reaction mixture. Flash column chromatography (ether) was used to give the product **7** (3.17 g, 55%). TLC (EtOAc-Hexane 1:1): R_f 0.40; ^{1}H-NMR ($CDCl_3$): δ 2.42 (3H, s, Ar-CH_3), 2.46 (3H, s, Ar-CH_3), 2.52 (1H, m, 2'-C*H*), 3.12 (1H, m, 2'-C*H*), 4.74 (3H, m, 5'-CH_2 and 4'-C*H*), 5.64 (1H, m,

3'-C*H*), 6.74 (1H, t, 1'-C*H*), 7.27 (4H, dd, 4 × Ar-*H*), 7.84 (2H, d, 2 × Ar-*H*), 7.97 (2H, d, 2 × Ar-*H*), 8.05 (1H, d, imidazole (4)-*H*), 8.11 (1H, s, imidazole (2)-*H*).

5-Amino-4-(2,2-dicyanovinyl)-1-(2-deoxy-3,5-di-*O*-*p*-toluoyl-β-D-ribofuranosyl)-imidazole 11

1-(2-Deoxy-3,5-di-*O*-*p*-toluoyl-β-D-ribofuranosyl)-5-nitroimidazole **6** (1.0 g, 2.17 mmol) and Pd (5%) on carbon (1.0 g) were placed in dry THF (40 mL). The mixture was hydrogenated (balloon) at atmospheric pressure, with vigorous shaking during 2 hours. TLC analysis (ether) showed disappearance of all starting material and a new baseline spot. The product mixture was filtered quickly through dry Celite under argon into a flask containing ethoxy methylene malononitrile (EMMN) (0.4 g, 3.3 mmol) and the reaction stirred at room temperature overnight to give a dark brown product solution. The solvent was removed under high vacuum at room temperature. The residue was treated with dry-ice chilled EtOAc (100 mL) and filtered to give 5-amino-4-(2,2-dicyanovinyl)-1-(2-deoxy-3,5-di-*O*-*p*-toluoyl-β-D-ribofuranosyl)-imidazole **11** as small needle-like yellow crystals (0.45 g, 43%). ^{1}H-NMR ($CDCl_3$): δ 2.39 (3H, s, Ar-CH_3), 2.41 (3H, s, Ar-CH_3), 2.72 (1H, m, 2'-C*H*), 2.86 (1H, m, 2'-C*H*), 4.53 (3H, m, 5'-CH_2 and 4'-C*H*), 5.63 (1H, d, 3'-C*H*), 6.09 (1H, dd, 1'-C*H*), 7.36 (4H, dd, 4 × Ar-*H*), 7.86 (2H, d, 2 × Ar-*H*), 7.95 (2H, d, 2 × Ar-*H*), 8.05 (1H, s, C=C-*H*), 8.83 (1H, s, imidazole(2)-*H*), 7.72 (2H, br s, NH_2, D_2O exchangeable).

5-Amino-6-cyano-3-(2-deoxy-β-D-ribofuranosyl)-imidazo[4,5-*b*]pyridine 12

5-Amino-4-(2,2-dicyanovinyl)-1-(2-deoxy-3,5-di-*O*-*p*-toluoyl-β-D-ribofuranosyl)-imidazole **11** (0.40 g, 0.78 mmol) was added to MeOH (40 mL), together with aqueous NaOH (1 g dissolved in water (5 mL)), and the mixture heated to reflux. The reaction was monitored by TLC (EtOAc-MeOH (10:1)) giving only one fluorescent spot with R_f = 0.3 after 15 minutes. The pH of the reaction solution was then carefully adjusted to pH 7 (indicator paper) by dropwise addition of 20% (aq) citric acid solution. The solution was filtered through Celite and the solvent removed under vacuum. The residue was purified by silica gel flash column chromatography eluting with EtOAc-MeOH (10:1) giving 5-amino-6-cyano-3-(2-deoxy-β-D-ribofuranosyl)-imidazo[4,5-*b*]pyridine **12** as a pale yellow solid. Recrystallization from water gave needle-like crystals (0.18 g, 84%). ^{1}H-NMR (d_6-DMSO): δ 2.23 (1H, m, 2'-C*H*), 2.59 (1H, m, 2'-C*H*), 3.52 (2H, m, 5'-CH_2), 3.83 (1H, d, 3'-C*H*), 4.37 (1H, s, 3'-C*H*), 4.96 (1H, t, 5'-O*H*), 5.32 (1H, d, 3'-O*H*), 6.29 (1H, t, 1'-C*H*), 6.79 (2H, br s, NH_2), 8.24 (1H, s, pyridine-*H*), 8.42 (1H, s, imidazole (2)-*H*).

6,8-Diamino-3-(2-deoxy-β-D-ribofuranosyl)-imidazo[4',5':5,6]pyrido[2,3-d] pyrimidine 13

Method A:

Guanidine hydrochloride (0.40 g, 4.2 mmol) was added to a solution of NaOMe (0.23 g, 4.2 mmol) in absolute MeOH (30 mL). The mixture was stirred at 20 to 23 °C for 15 min before 5-amino-6-cyano-3-(2-deoxy-β-D-ribofuranosyl)-imidazo[4,5-*b*]pyridine **12** (0.10 g, 0.36 mmol) was added.

After a 42 h stirring in 145 °C, TLC (EtOAc-MeOH, 10:1) showed absence of **12**. The solid filtered from the cooled mixture was washed successively with H_2O and EtOH to yield **13** (0.52 g, 45%).

Method B:

Guanidine hydrochloride (0.41 g, 4.2 mmol) was added to a solution of NaOMe (0.25 g, 4.3 mmol) in absolute MeOH (30 mL). The mixture was stirred at 20 to 23 °C for 15 min and filtered to remove the NaCl salt before 5-amino-6-cyano-3-(2-deoxy-β-D-ribofuranosyl)-imidazo[4,5-*b*]pyridine **12** (0.10 g, 0.36 mmol) was added. After a 72 h stirring in 120 °C with reflux, TLC (EtOAc-MeOH, 10:1) showed absence of **12**. The solid filtered from the cooled mixture was washed EtOH to yield **13** (0.23 g, 19%).

Mp > 280 °C IR (KBr): ν_{max} 803, 1057, 1356, 1470, 1621, 2887, 3110, 3183, 3318, 3434, 3481 cm^{-1}. ^{1}H-NMR (d_6-DMSO): δ 2.23 (1H, m, 2'-C*H*), 2.81 (1H, m, 2'-C*H*), 3.61 (2H, m, 5'-CH_2), 3.88 (1H, m, 4'-C*H*), 4.44 (1H, m, 3'-C*H*), 5.17 (1H, t, 5'-O*H*), 5.37 (1H, d, 3'-O*H*), 6.19 (2H, br s, NH_2), 6.42 (1H, t, 1'-C*H*), 7.44 (2H, br s, NH_2), 8.64 (1H, s, 6-*H*), 8.83 ppm (1H, s, 9-*H*). ^{13}C-NMR (d_6-DMSO): δ 39.17 (t, 2'-*C*H_2), 62.08 (t, 5-*C*H_2), 71.17 (d, 4'-*C*H), 83.84 (d, 3'-*C*H), 88.01 (d, 1'-CH), 102.19 (s, *C*), 123.83 (d, *C*H), 131.33 (s, *C*), 145.35 (d, *C*H), 150.76 (s, *C*), 158.27 (d, *C*H), 162.78 (s, *C*), 164.21 (s, *C*). MS (FAB): *m/z* (%) 318(91) [M + H], 202(100), 141(15), 121(9). HRMS-FAB: *m/z* calcd for $C_{13}H_{15}N_7NaO_3$: 340.1134. Found 340.1129 [M^+ + Na].

5-Amino-3-(2-deoxy-β-D-ribofuranosyl)-imidazo[4,5-*b*]pyridine-6-carboxylic acid amide 14

5-Amino-6-cyano-3-(2-deoxy-β-D-ribofuranosyl)-imidazo[4,5-*b*]pyridine **12** (0.18 g, 0.65 mmol), NH_4OH (4 mL), and 35% H_2O_2 (1.2 mL) was stirred at rt (40 min). The mixture was then refrigerated overnight and the colourless solid product was collected and recrystallised from EtOH to afford compound **14** as colourless needles (0.11 g, 57%). ^{1}H-NMR (d_6-DMSO): δ 2.23 (1H, m, 2'-C*H*), 2.59 (1H, m, 2'-C*H*), 3.43 (2H, m, 5'-CH_2), 3.82 (1H, d, 4'-C*H*), 4.37 (1H, d, 3'-C*H*), 5.02 (1H, t, 5'-O*H*), 5.31 (1H, d, 3'-O*H*), 6.30 (1H, t, 1'-C*H*), 7.33 (2H, br s, NH_2), 8.30 (1H, s, pyridine-*H*), 8.34 (1H, s, imidazole (2)-*H*).

References

1. Watson, J.D.; Crick, F.H.C. *Nature* **1953**, *171*, 737

2. Avery, O.T.; MacLeod, C.M.; McLarty, M. *J. Exp. Med.* **1944**, *79*, 137

3. Uhlmann, E.; Peyman, A. *Chem. Rev.* **1990**, *90*, 543

4. Cook, P.D. *Anticancer Drug Res.* **1991**, *6*, 585

5. Thoung, N.G.; Hélène, C. *Angew. Chem. Int. Ed. Engl.* **1993**, *32*, 666

6. Sun, J.-S.; Garestier, T.; Hélène, C. *Curr. Opin. Struct. Biol.* **1996**, *6*, 327

7. Dervan, P.B.; Moser, H.E. *Science* **1987**, *238*, 645

8. Hélène, C.; Le Doan T.; Perrouadt, L.; Proseuth D.; Habhoub N.; Decout, J.-L.; Thoung, N.T.; Homme, J.L. *Nucleic Acids Res.* **1987**, *15*, 7749

9. Colocci, N.; Devan, P.B. *J. Am. Chem. Soc.* **1994**, *116*, 785

10. Froehler, B.C.; Wadwani, S.; TerHorst, T.J.; Gerrard, S.R. *Tetrahedron Lett.* **1992**, *33*, 5307

11. Phipps, A.K.; Tarkoy, M.; Shultze, P.; Feigon, *Biochemistry* **1998**, *37*, 5820

12. Posvic, T.J.; Devan, P.B. *J. Am. Chem. Soc.* **1989**, *111*, 3059

13. Verma, S.; Miller, P.S. *Bioconjugate Chem.* **1996**, *7*, 600

14. Zamecnik, P.C.; Stephenson, M.L. *Proc. Natl. Acad. Sci. USA* **1978**, *75*, 280

15. Stephenson, M.L.; Zamecnik, P.C. *Proc. Natl. Acad. Sci. USA* **1978**, *75*, 285

16. Ratajczak, M.Z.; Kant, J.A.; Luger, S.M.; Hijiya, N.; Zhang, J.; Zon, G.; Gewirtz, A.M. *Proc. Natl. Acad. Sci. USA* **1992**, *89*, 11823

17. Vander Krol, A.R.; Mel, J.N.M.; Stuitje, A.R. *Gene* **1988**, *72*, 45

18. Hjalt, T.; Wagner, E.G.H.; *Nucleic Acids Res.* **1992**, *20*, 6723

19. Hjalt, T.; Wagner, E.G.H.; *Nucleic Acids Res.* **1995**, *23*, 580

20. Crooke, S.T. *Ann. Rev. Pharmacol. Toxicol.* **1992**, *32*, 329

21. Leonetti, J.P.; Degols, C.; Clarenc, J.P.; Mechti, N.; Lebleu, B. *Prog. Mol. Biol.* **1993**, *44*, 143

22. Neckers, L.; Whitsell, L.; Rosolen, A.; Geselwitz, D.A. *Crit. Rev. Oncog.* **1992**, *3*, 175

23. Boiziau, C.; Kufurst, R.; Cazenave, C.; Roig, V.; Thuong, N.T.; Toulme, J.-J. *Nucleic Acids Res.* **1991**, *19*, 1113

24. Shakin, S.H.; Liebhaber, S.A. *J. Biol. Chem.* **1986**, *261*, 16018

25. Haeuptle, M.T.; Frank, R.; Dobberstein, B. *Nucleic Acids Res.* **1986**, *14*, 1427

26. Minshull, J.; Hunt, T. *Nucleic Acids Res.* **1986**, *14*, 6433

27. Ogawa, T.; Pickett, G.G.; Kogoma, T.; Kornberg, A. *Proc. Natl. Acad. Sci. USA* **1984**, *81*, 1040

28. Kogoma, T.; Subia, N.L.; Meyenberg, K. *Mol. Gen. Genet.* **1985**, *200*, 103

29. Horiuchi, T.; Maki, H.; Sekiguchi, M. *Mol. Gen. Genet.* **1985**, *195*, 17

30. Lisa, D.C.; David, Y.B.; Kevin, J.S. *Pharmacol. Ther.* **1997**, *74*, 317

31. Temsamani, J.; Tang, J.-Y.; Padmapriya, A.; Kubert, M.; Agrawal, S. *Antisense Res. Dev.* **1993**, *3*, 277

32. Nicklin, P.L.; Ambler, J.; Mitchelson, A.; Bayley, D.; Philips, J.A.; Craig, S.J.; Monia, B.P. *Proc. Natl. Acad. Sci. USA* **1997**, *16*, 1145

33. Shaw, J.-P.; Kent, K.; Fishback, J.; Fröehler, B. *Nucleic Acids Res.* **1991**, *19*, 747

34. Gao, W.Y; Storm, C.; Egan, W.; Cheng, Y.C. *Mol. Pharmacol.* **1993**, *43*, 45

35. Wallase, T.L.; Bazemore, S.A.; Kornbrust, D.J.; Cossum, P.A. *J. Pharmacol. Exp. Ther.* **1996**, *278*, 1306

36. Cech, T.R.; Zaug, A.J.; Grabowski, P.J. *Cell* **1981**, *27*, 487

37. Kruger, K.; Grabowski, P.J.; Zaug, A.J.; Sands, J.; Gottschling, D.E.; Cech, T.R. *Cell* **1982**, *31*, 147

38. Guerrier-Takada, C.; Gardiner, K.; Marsh, T.; Pace, N.; Altman, S. *Cell* **1983**, *35*, 849

39. Buzayan, J.M.; Feldstein, P.A.; Bruening, G.; Eckstein, F. *Biochem. Biophys. Res. Commun.* **1988**, *156*, 340

40. Noller, H.F.; Ho¡arth, V.; Zimniak, L. *Science* **1992**, *256*, 1416

41. Nitta, I.; Kamada, Y.; Noda, H.; Ueda, T.; Watanabe, K. *Science* **1998**, *281*, 666

42. Uhlenbeck, O.C. *Nature* **1987**, *328*, 596

43. Hampel, A.; Tritz, R.; Hicks, M.; Cruz, P. *Nucleic Acids Res.* **1990**, *18*, 299

44. Kijima, H.; Ishida, H.; Ohkawa, T.; Kashani-Sabet, M.; Scanlon, K.J. *Pharmacol. Ther.* **1995**, *68*, 247

45. Symons, R.H. *Curr. Opin. Struct. Biol.* **1994**, *4*, 322

46. Symons, R.H. *Nucleic Acids Res.* **1997**, *25*, 2683

47. Narlikar, G.J.; Herschlag, D. *Ann. Rev. Biochem.* **1997**, *66*, 19

48. Steitz, T.A.; Steitz, J.A. *Proc. Natl. Acad. Sci. USA* **1993**, *90*, 6498

49. Walter, N.G.; Burke, J.M. *Curr. Opin. Struct. Biol.* **1998**, *2*, 24

50. Felsenfeld, G.; Rich, A. *Biochem. Biophys. Acta* **1957**, *26*, 457

51. Felsenfeld, G.; Davies, D.R.; Rich, A. *J. Am. Chem. Soc.* **1957**, *79*, 2023

52. Riley, M.; Maling, B.; Chamberlin, M.J. *J. Mol. Biol.* **1966**, *20*, 359

53. Morgan, A.R.; Well, R.D. *J. Mol. Biol.* **1968**, *37*, 63

54. Lee, J.S.; Johnson, D.A.; Morgan, A.R. *Nucleic Acids Res.* **1979**, *6*, 3073

55. Lyamichev, V.I.; Mirkin, S.M.; Frank-Kamenetskii, M.D. *J. Biomol. Struct. Dyn.* **1986**, *3*, 667

56. Mirkin, S.M.; Lyamichev, V.I.; Drushlyak, K.N.; Dobrynin, V.N; Filippov, S.A.; Frank-Kamenetskii, M.D. *Nature* **1987**, *330*, 495

57. Le Doan, T.; Perrouault, L.; Praseuth, D.; Habhoub, N.; Decout, J.L.; Thoung, T.; Lhomme, J.; Hélène, C. *Nucleic Acids Res.* **1987**, *15*, 7749

58. Lyamichev, V.I.; Mirkin, S.M.; Frank-Kamenetskii, M.D.; Cantor, C.R. *Nucleic Acids Res.* **1988**, *16*, 2165

59. Gowers, D.M.; Fox, K.R. *Nucleic Acids Res.* **1999**, *27*, 1569

60. Johnston, B.H. *Science* **1988**, *241*, 1800

61. Letai, A.G.; Palladino, M.A.; Fromm, E.; Rizzo, V.; Fresco, J.R. *Biochemistry* **1988**, *28*, 3860

62. Svinarchuk, F.; Bertrand, J.-R.; Malvy, C. *Nucleic Acids Res.* **1994**, *22*, 3742

63. Svinarchuk, F.; Paoletti, J.; Malvy, C. *J. Biol. Chem.* **1995**, *270*, 14068

64. Fox, K.R. *Nucleic Acids Res.* **1994**, *22*, 2016

65. Chandler, S.P.; Fox, K.R. *Biochemistry* **1996**, *35*, 15038

66. Brown, P.M.; Madden, C.A.; Fox, K.R. *Biochemistry* **1998**, *37*, 16139

67. Brown, P.M.; Fox, K.R. *Biochem. J.* **1996**, *319*, 607

68. Noonberg, S.B.; François, J.-C.; Garestier, T.; Hélène, C. *Nucleic Acids Res.* **1995**, *23*, 1956

69. Mergny, J.-L.; Sun, J.-S.; Rougee, M.; Montenay-Garesteir, T.; Barcelo, F.; Chomilier, J. and Hélène, C. *Biochemistry* **1991**, *30*, 9791

70. Maher, L.J.; Wold, B.; Dervan, P.B. *Science* **1989**, *245*, 725

71. Maher, L.J.; Dervan, P.B.; Wold, B. *Biochemistry* **1992**, *31*, 70

72. Lee, J.S.; Wordsworth, M.L.; Latimer, L.J.P.; Morgan, A.R. *Nucleic Acids. Res.* **1984**, *12*, 6603

73. Roberts, R.W.; Crothers, D.M. *Proc. Natl. Acad. Sci. U.S.A.* **1996**, *93*, 4320

74. Xodo, L.E.; Manzini, G.; Quadrifoglio, F.; van der Marel, G.; van Boom, J. *Nucleic Acids Res.* **1991**, *19*, 5625

75. Xiang, G.; Bogacki, R.; McLaughlin, L.W. *Nucleic Acids Res.* **1996**, *24*, 1963

76. Ono, A.; Ts'o, P.O.P.; Kan, L. *J. Am. Chem. Soc.* **1991**, *113*, 4032

77. Berressem, R.; Engels, J.W. *Nucleic Acids Res.* **1995**, *23*, 3465.

78. Von Krosigk, U.; Benner, S.A. *J. Am. Chem. Soc.* **1995**, *117*, 5361

79. Bates, P.J.; Laughton, C.A.; Jenkins, T.C.; Capaldi, D.C.; Roselt, P.D.; Reese, C.B; Neidle, S. *Nucleic Acids Res.* **1996**, *24*, 4176

80. Hildbrand, S.; Blaser, A.; Parel, S.P.; Leumann, C.J. *J. Am. Chem. Soc.* **1997**, *119*, 5499

81. Cassidy, S.A.; Slickers, P.; Trent, J.O.; Capaldi, D.C.; Roselt, P.D.; Reese, C.B.; Neidle, S.; Fox, K.R. *Nucleic Acids Res.* **1997**, *25*, 4891

82. Koh, J.S.; Dervan, P.B. *J. Am. Chem. Soc.* **1992**, *114*, 1470

83. Radhakrishnan, I.; Patel, D.J.; Priestley, E.S.; Nash, H.M.; Dervan, P.B. *Biochemistry* **1993**, *32*, 11228

84. Priestley, E.S.; Dervan, P.B. *J. Am. Chem. Soc.* **1995**, *117*, 4761

85. Miller, P.S.; Bhan, P.; Cushman, C.D.; Trapane, T.L. *Biochemistry* **1992**, *31*, 6788

86. Rao, T.S.; Hogan, M.E.; Revankar, G.R. *Nucleosides Nucleotides* **1994**, *13*, 95

87. Milligan, J.F.; Krawczyk, S.H.; Wadwani, S.; Matteucci, M.D. *Nucleic Acids Res.* **1993**, *21*, 327

88. Roig, V.; Kurfurst, R.; Thuong, N.T. *Tetrahedron Lett.* **1993**, *34*, 1601

89. Rao, T.S.; Lewis, A.F.; Durland, R.S.; Revankar, G.R. *Tetrahedron Lett.* **1993**, *34*, 6709

90. Chaturvedy, S.; Horn, T.; Letsinger, R.L. *Nucleic Acids Res.* **1996**, *24*, 2318

91. Gryaznov, S.; Lloyd, D.H.; Chen, J.K.; Schultz, R.G.; DeDionisio, L.A.; Ratmeyer, L.; Wilson, W.D. *Proc. Natl. Acad. Sci. USA* **1995**, *92*, 5798

92. Dueholm, K.L.; Nielsen, P.E. *New J. Chem.* **1997**, *21*, 19

93. Eckstein, F. *J. Am. Chem. Soc.* **1966**, *88*, 4292

94. Eckstein, F. *Ann. Rev. Biochem.* **1985**, *54*, 367

95. Latimer, L.; Hampel, K.; Lee, J.S. *Nucleic Acids Res.* **1989**, *17*, 1549

96. Xodo, L.; Alunni-Fabbroni, M.; Manzini, G.; Quadrifoglio, F. *Nucleic Acids Res.* **1994**, *22*, 3322

97. Hacia, J.G.; Wold, B.J.; Dervan, P.B. *Biochemistry* **1994**, *33*, 5367

98. Joseph, J.; Kandala, J.; Veerapanane, D.; Weber, K.; Guntaka, R. *Nucleic Acids Res.* **1997**, *25*, 2182

99. Faruqi, A.F.; Krawczyk, S.H.; Matteucci, Glazer, P.M. *Nucleic Acids Res.* **1997**, *25*, 633

100. Svinarchuk, F.; Debin, A.; Bertrand, J.R.; Malvy, C. *Nucleic Acids Res.* **1996**, *24*, 295

101. Tu, G.C.; Cao, Q.N.; Israel, Y. *J. Biol. Chem.* **1995**, *270*, 28402

102. Guvakova, M.A.; Yabukov, L.A.; Vlodavsky, I.; Tonkinson, J.L.; Stein, C.A. *J. Biol. Chem.* **1995**, *270*, 2620

103. Kim, S.G.; Tsukahara, S.; Yokoyama, S.; Takaku, H.; *FEBS Lett.* **1992**, *314*, 29

104. Miller, P.S.; Yano, J.; Yano, E.; Carrol, C.; Jayraman, K.; Ts'o, P.O.P. *Biochemistry* **1979**, *18*, 5134

105. François, J.-C.; Saison-Behmoaras, T.; Barbier, C.; Chassignol, M.; Thuong, N.T.; Hélène, C. *Proc. Natl. Acad. Sci. USA* **1989**, *86*, 9702

106. François, J.-C.; Saison-Behmoaras, T.; Chassignol, M.; Thuong, N.T.; Hélène, C. *J. Biol. Chem.* **1989**, *264*, 5891

107. Kibler-Herzog, L.; Kell, B.; Zon, G.; Whittier, G.; Shinozuka, K.; Mizan, S.; Wilson, W.D. *Nucleic Acids Res.* **1990**, *18*, 3534

108. Ray, A.; Nordén, B. *FASEB* **2000**, *14*, 1041

109. Egholm, M.; Buchardt, O.; Christensen, L.; Behrens, C.; Frier, S.M.; Driver, D.A.; Berg, R.H.; Kim, S.K.; Nordén, B.; Nielsen, P.E. *Nature (London)* **1993**, *365*, 566

110. Nielsen, E.; Christensen, L. *J. Am. Chem. Soc.* **1996**, *118*, 2287

111. Giovannangeli, C.; Perroult, L.; Escudé, C.; Gryaznov, S.; Charneau, P.; Hélène, C. *J. Mol. Biol.* **1996**, *261*, 386

112. Giovannangeli, C.; Diviacco, S.; Labrousse, V.; Gryaznov, S.; Charneau, P.; Hélène, C. *Proc. Natl. Acad. Sci. USA* **1997**, *94*, 79

113. Gryaznov, S.; Chen, J.K. *J. Am. Chem. Soc.* **1994**, *116*, 3143

114. Chen, J.K.; Schultz, R.G.; Lloyd, D.H.; Gryaznov, S. *Nucleic Acids Res.* **1995**, *23*, 2661

115. Tereshko, V.; Gryaznov, S.; Megli, M. *J. Am. Chem. Soc.* **1998**, *120*, 269

116. Semerad, L.J.; Maher III. *Nucleic Acids Res.* **1994**, *22*, 5321

117. Sun, J.; Garestier, T.; Hélène, C. *Curr. Opin. Struct. Biol.* **1996**, *6*, 327

118. Thuong, N.T.; Hélène, C. *Angew. Chem. Int. Ed. Engl.* **1993**, *32*, 666

119. Gotfredsen, C.; Schultze, P.; Feigon, J. *J. Am. Chem. Soc.* **1998**, *120*, 4281

120. Kandimalla, E.; Venkataraman, G.; Sasisekharan, V.; Agrawal, S. *J. Biomol. Struct. Dyn.* **1997**, *14*, 715

121. Han, H.; Devan, P.B. *Proc. Natl. Acad. Sci. USA* **1993**, *90*, 3806

122. Cuenoud, B.; Casset, F.; Hüsken, D.; Natt, F.; Wolf, R.; Altmann, K.; Martin, P.; Moser, H. *Angew. Chem. Int. Ed. Engl.* **1998**, *37*, 1288

123. Jones, G.D.; Altmann, K.H.; Hüsken, D.; Walker, R.T. *Bio. & Med. Chem. Lett.* **1997**, *7*, 1275

124. Froehler, B.C. and Ricca, D.J. *J. Am. Chem. Soc.* **1992**, *114*, 8320

125. Asseline, U.; Thuong, N.T.; Hélène, C. *New J. Chem.* **1997**, *21*, 5

126. Garbesi, A.; Bonazzi, S.; Zanella, S.; Capobianco, M.L.; Giannini, G.; Arcamone, F. *Nucleic Acids Res.* **1997**, *25*, 2121

127. Mergny, J.L.; Duval-Valentin, G.H.; Perrouault, L.; Faucon, B.; Rougée, M.; Montenay-Garestier, T.; Nisagni, E.; Hélène, C. *Science* **1992**, *256*, 1681

128. Escudé, C.; Nguyen, C.H.; Mergny, J.L.; Sun, J.S. Bisagni, E.; Garestier, T.; Hélène, C. *J. Am. Chem. Soc.* **1995**, *117*, 10212

129. Robles, J.; Rajur, S.B.; McLaughlin, L.W. *J. Am. Chem. Soc.* **1996**, *118*, 5820

130. Szewcyk, J.W.; Baird, E.E.; Dervan, P.B. *Angew. Chem. Int. Ed. Engl.* **1996**, *35*, 1487

131. Tung, C.H.; Breslauer, K.J.; Stein, S. *Nucleic Acids Res.* **1993**, *21*, 5489

132. Rajeev, K.G.; Jadhav, V.R.; Ganesh, K.N. *Nucleic Acids Res.* **1997**, *25*, 4187

133. Tung, C.H.; Breslauer, K.J.; Stein, S. *Bioconjugate Chem.* **1996**, *7*, 529, 531

134. Sergeyev, D.S.; Godovikova, T.S.; Zarytova, V.F. *Nucleic Acids Res.* **1995**, *23*, 4400

135. Lukhtanov, E.A.; Mills, A.G.; Kutyavin, I.V.; Gorn, V.V.; Reed, M.W.; Meyer, R.B. *Nucleic Acids Res.* **1997**, *25*, 5077

136. Matteucci, M.; Lin, K.Y.; Huang, T.; Wagner, R.; Sternbach, D.D.; Mehrota, M.; Besterman, J.M. *J. Am. Chem. Soc.* **1997**, *119*, 6939

137. Bates, P.J.; Laughton, C.A.; Jenkins, T.C.; Capaldi, D.C.; Roselt, P.D.; Reese, C.B.; Neidle, S. *Nucleic Acids Res.* **1996**, *24*, 4176

138. Faucon, B.; Mergny, J.-L.; Hélène, C. *Nucleic Acids Res.* **1996**, *24*, 3181

139. Clayton, R.; Davis, M.L.; Fraser, W.; Li, W.; Ramsden, C.A. *Synlett.* **2002**, 1483

140. Lin, K.-Y.; Jones, R.J.; Matteucci, M. *J. Am. Chem. Soc.* **1995**, *117*, 3873

141. Kazimierczuk, Z.; Cottam, H.B.; Revankar, G.R.; Robins, R.K. *J. Am. Chem. Soc.* **1984**, *106*, 6379

142. Winkeler, H.-D.; Seela, F. *J. Org. Chem.* **1983**, *48*, 3119

143. Lythgoe, D.J.; Ramsden, C.A. *Adv. Heterocycl. Chem.* **1994**, *61*, 1

144. Humphries, M.J.; Ramsden, C.A. *Synlett.* **1995**, 203

145. Bergstrom, D.E.; Zhang, P.; Johnson, W.T. *Nucleic Acids Res.* **1997**, *25*, 1935

146. Štimac, A.; Kobe, J. *Carbohydrate Res.* **2000**, *329*, 317

147. Hubbard, A.J.; Jones, A.S.; Walker, R.T. *Nucleic Acids Res.* **1984**, *12*, 6827

148. Humphries, M.J.; Ramsden, C.A. *Synthesis* **1999**, 985

149. Al-Shaar, A.H.M.; Gilmour, D.W.; Lythgoe, D.J.; McClenaghan, I.; Ramsden, C.A. *J. Chem. Soc., Perkin Trans. 1* **1992**, 2779

150. DeGraw, J.I.; Tagawa, H. *J. Heterocycl. Chem.* **1982**, *19*, 1461

151. Piper, J.R.; McCaleb, G.S.; Maddry, J.A.; Malik, N.D.; McGuire, J.J.; Otter, G.M.; Sirotnak, F.M. *J. Med. Chem.* **1993**, *36*, 4161

152. Taylor E.C. *J. Heterocycl. Chem.* **1990**, *27*, 1

153. Piper, J.R.; Montgomery, J.A. *J. Org. Chem.* **1977**, *42*, 208

154. Piper, J.R.; Montgomery, J.A. *J. Heterocycl. Chem.* **1974**, *11*, 279

155. Hirota, K.; Watanabe, K.A.; Fox, J.J. *J. Heterocycl. Chem.* **1977**, *14*, 537

156. Hirota, K.; Watanabe, K.A.; Fox, J.J. *J. Org. Chem.* **1978**, *43*, 1193

157. Pankiewicz, K.; Matsuda, A.; Watanabe, K.A. *J. Org. Chem.* **1982**, *47*, 485

158. Lessor, R.A.; Leonard, N.J. *J. Org. Chem.* **1981**, *46*, 4300

159. Leonard, N.J.; Hiremath, S.P. *Tetrahedron* **1986**, *42*, 1917

160. Poushin, N.N.; Cohen, J.S. *Nucleic Acids Res.* **1994**, *22*, 5492

161. Still, W.C.; Kahn, M.; Mitra, A. *J. Org. Chem.* **1978**, *43*, 2923

Appendix